



17<sup>TH</sup> ADVANCED BEAM DYNAMICS WORKSHOP ON

## **FUTURE LIGHT SOURCES**

# X-ray Optics

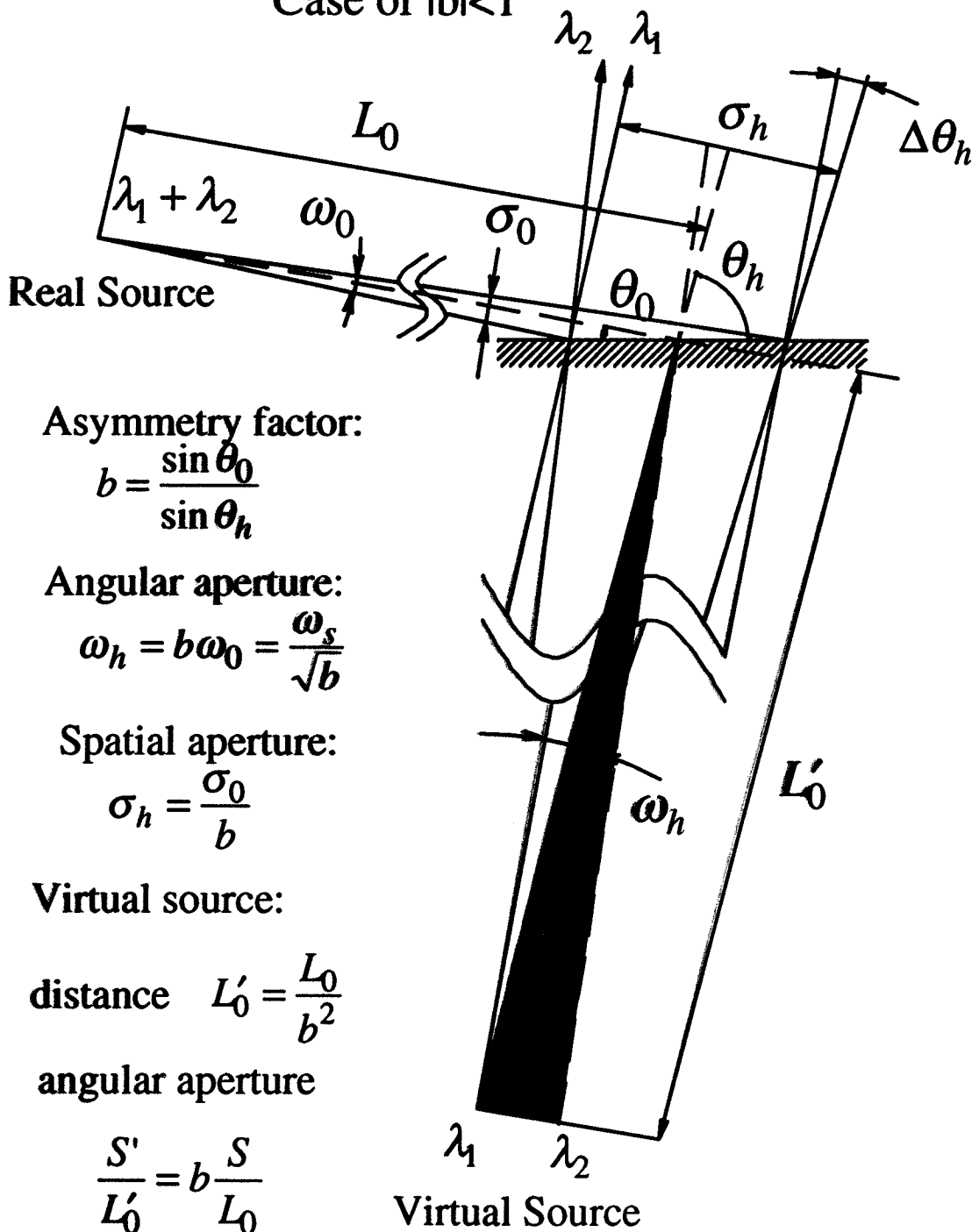
*A. Freund, ESRF*

APRIL 6-9, 1999

ARGONNE NATIONAL LABORATORY, ARGONNE, IL U.S.A.

# Optical Properties of a Single Asymmetrically Cut Crystal

Case of  $|b| < 1$



Courtesy: A. SOUVOROV (ESRF)

# EXAMPLES : Si AND DIAMOND AT $1.5\text{\AA}$ \*

Crystal	$d(\text{\AA})$	$\theta_B$	$\theta_i$	$\theta_e$	$b$	foot-print (mm)	$\Delta E/E$	$t_{ext}(\mu\text{m})$	$t_{abs}(\mu\text{m})$
Si(220)	1.9200	$22.99^\circ$	$0.1^\circ$	$45.88^\circ$	411	85.9	$1.2 \times 10^{-3}$	0.10	$3 \cdot 10^{-4} 0.124$
C*(111)	2.0593	$21.36^\circ$	$0.1^\circ$	$42.62^\circ$	388	85.9	$1.2 \times 10^{-3}$	0.11	0.65 2.33



Power spreading factor :  $\approx 600$ !



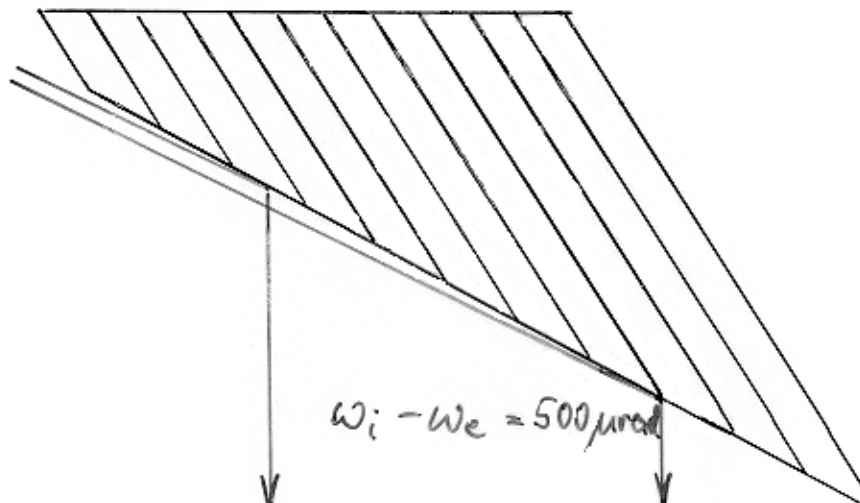
full range reflected

Surface should be very smooth and precisely oriented : feasible !

\* No refraction corrections of the Bragg angle included.

Further possibilities:

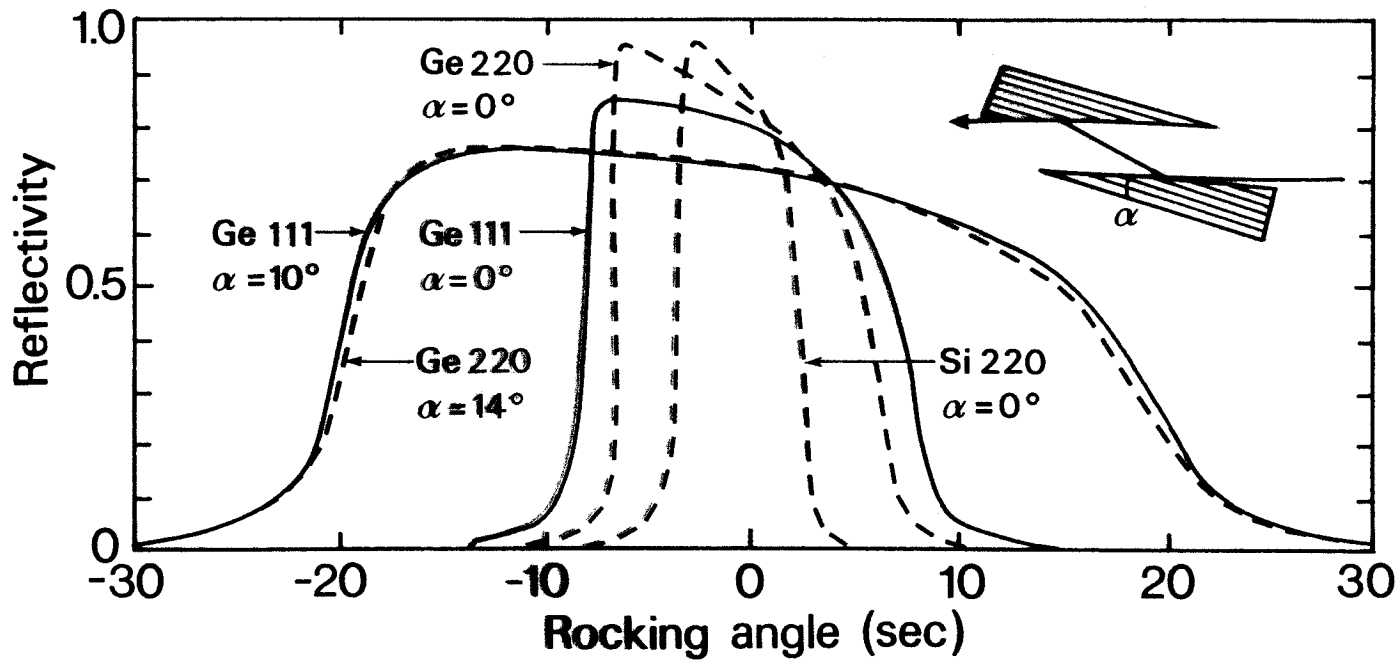
- inclined geometry
- Borrmann effect  
(anomalous transmission)
- long beamlines



From:

A. Freund

SLAC Workshop (1997)



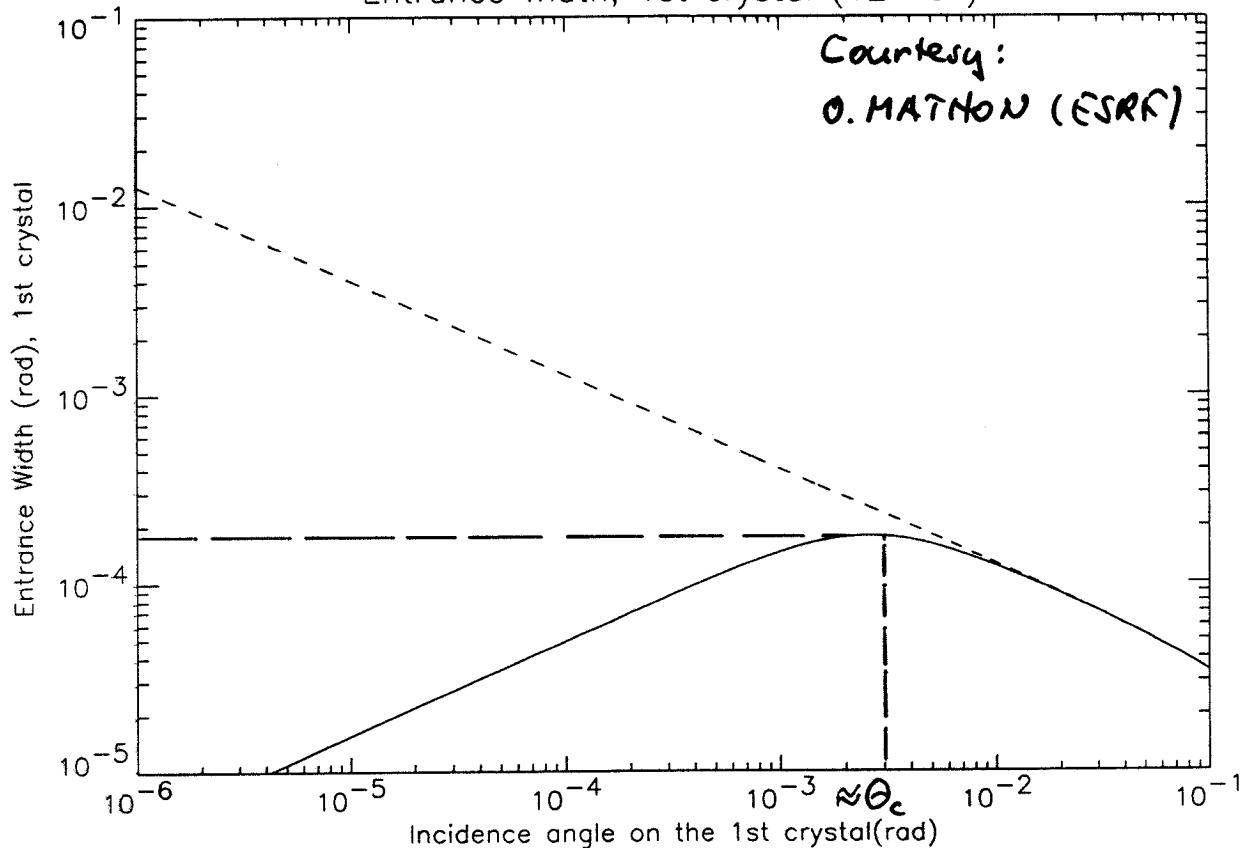
From: MATSUSHITA & HASHIZUME (1983)

Si(111)

Entrance Width, 1st crystal (12 KeV)

Courtesy:

O. MATTON (ESRF)



Symmetric

$$\omega_D = \frac{\Delta E}{E} \tan \theta = 2.3 \times 10^{-5} \text{ rad} \quad \frac{\Delta E}{E} = 1.4 \times 10^{-4}$$

Asymmetric

$$\omega_{A,i} = \omega_D / \sqrt{5}; \text{ max : } 2 \times 10^{-4} \text{ rad} \quad \left( \frac{\Delta E}{E} \right)_{\text{max}} = 1.4 \times 10^{-3}$$

$$b = \frac{\sin \theta - \alpha}{\sin \theta + \alpha} \Rightarrow b_{\min} \approx \frac{1}{100}$$

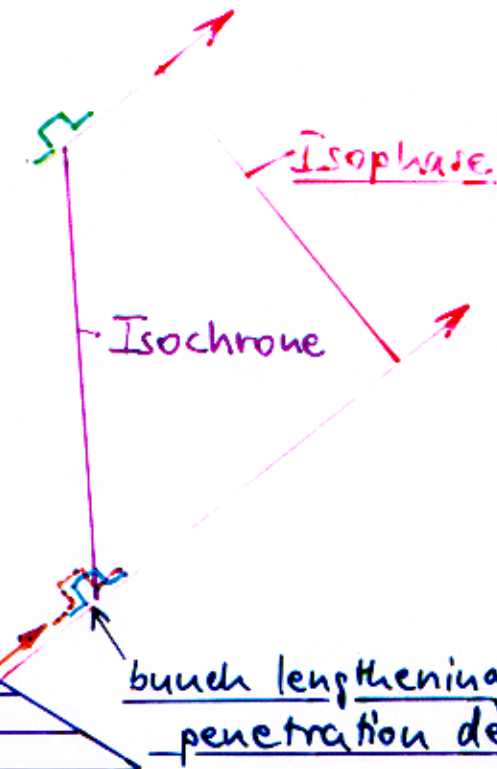
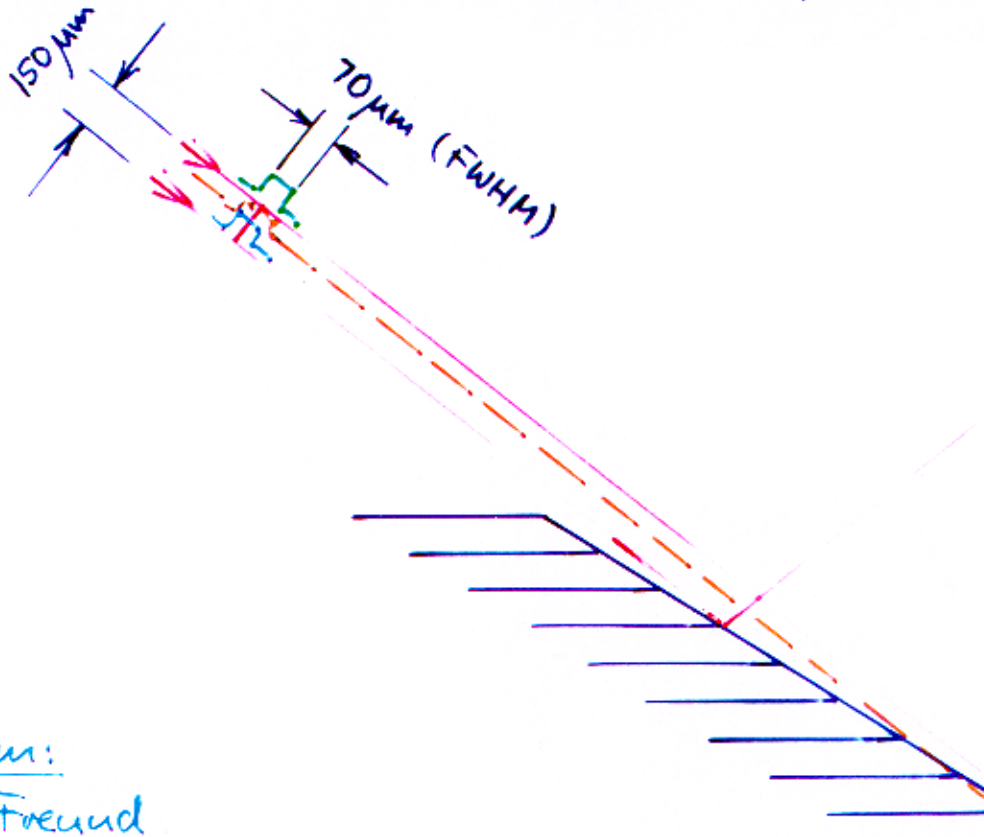
$$\omega_{A,e} = \omega_D \sqrt{5}; \text{ min } = 2 \times 10^{-6} \text{ rad};$$

## ISOPHASES AND ISOCHRONES

### Possibilities:

- Time dispersion
- Time focusing
- Bunch lengthening
- Bunch compression

} In connection with:  
- Time-Energy dependence of source  
- Gradient crystals



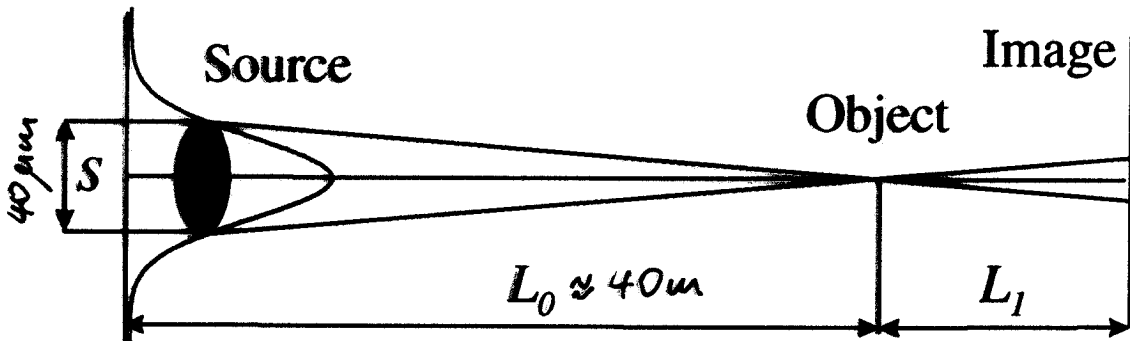
From:

A. Foernd

SLAC Workshop (1997)

bunch lengthening due to  
penetration depth effect:  $\approx 10^4$

# Introduction



While distance  $L_0$  is large,

COHERENCE → SPATIAL + TEMPORAL

SPATIAL COHERENCE  
is inverse to the source size

$$\propto \frac{\lambda}{S} L_0 \approx 100 \mu\text{m}$$

TEMPORAL COHERENCE  
is inverse to the spectral width

$$\propto \frac{\lambda^2}{\Delta\lambda}$$

Can we control coherence?

TEMPORAL COHERENCE → crystal monochromators  
provide  $\Delta\lambda/\lambda \sim 10^{-4}-10^{-6}$

SPATIAL COHERENCE → distance, filters, mirrors

The suitability of asymmetrically cut crystals  
to control spatial coherence:

true or false ?

Courtesy: A. SOUVOROV (ESRF)

# Requirements on quality of monochromators

## II. Tolerance on miscut in (+,-) asymmetrical reflection

$$|\Delta\varphi| = \frac{\eta\omega_s \sin^2(\theta_B - \varphi)}{\sqrt{b_1}\omega_c \sin 2\theta_B}$$

Example:

The same parameters as before, plus  
 $\varphi=8.48^\circ$  which gives  $b_1=4\cdot10^{-2}$ ,  $b_2=25$   
Then

$$|\Delta\varphi| < 10^{-5} \text{ rad (which is } \sim 2''\text{)}$$

## III. Tolerance on temperature difference in (+,-) asymmetrical reflection

$$|\Delta T| \leq \frac{\eta\omega_s \sin^2(\theta_B - \varphi)}{\alpha_T \sqrt{b_1}\omega_c \sin 2\varphi \tan \theta_B}$$

Example:

The same parameters as before, plus  
 $\alpha_T=2.5\cdot10^{-6} \text{ K}^{-1}$

Then

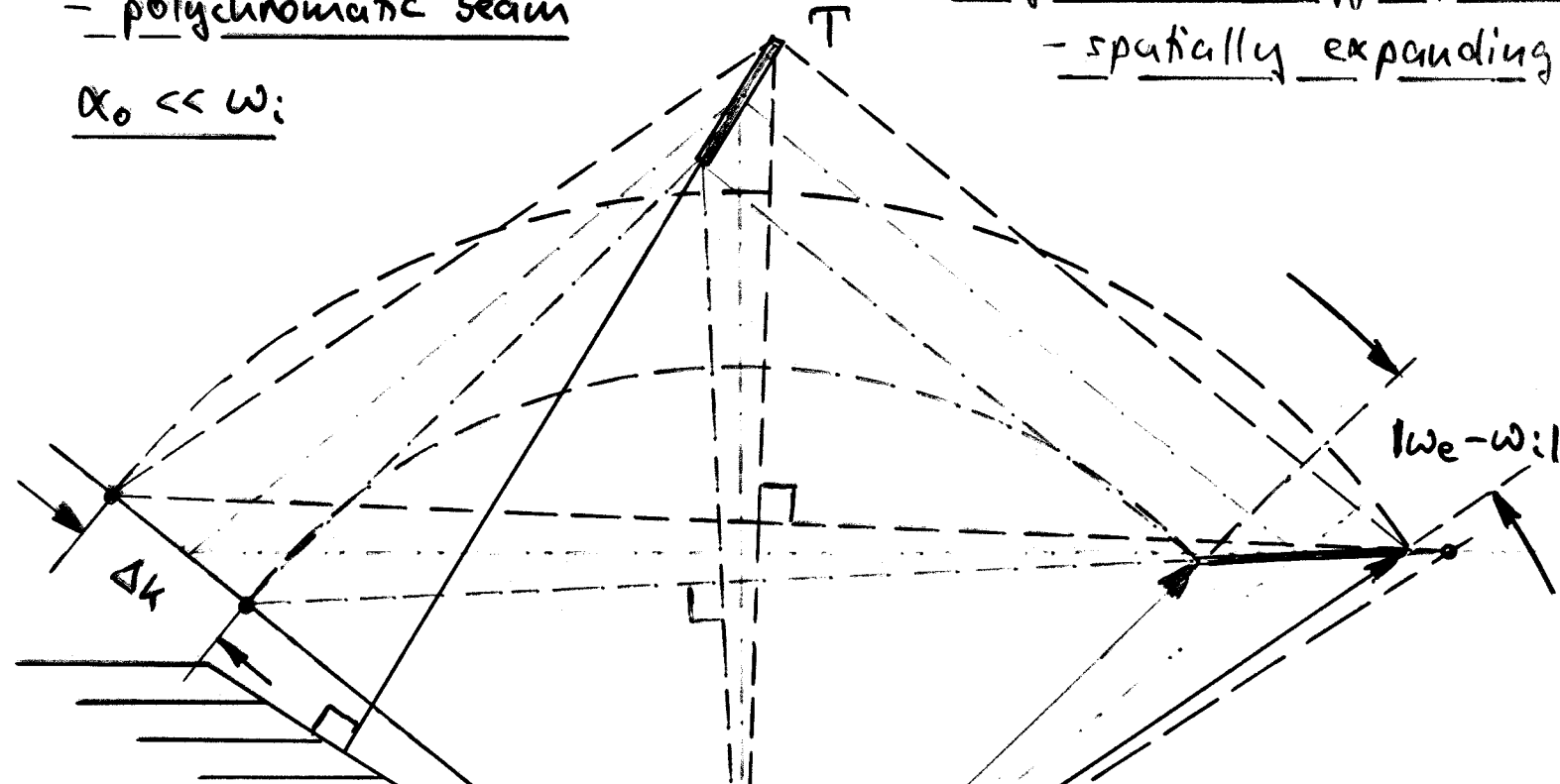
$$|\Delta T| < 30^\circ$$

Courtesy: A. SOUVOROV (ESRF)

# RECIPROCAL SPACE DIAGRAM

- polychromatic beam

$$\alpha_0 \ll w_i$$



$$\frac{\Delta k}{k} \approx w_i \cot \theta_B$$

Asymmetric Bragg reflection

- spatially expanding case

# SOME CRYSTAL PARAMETERS AT 8 KEV

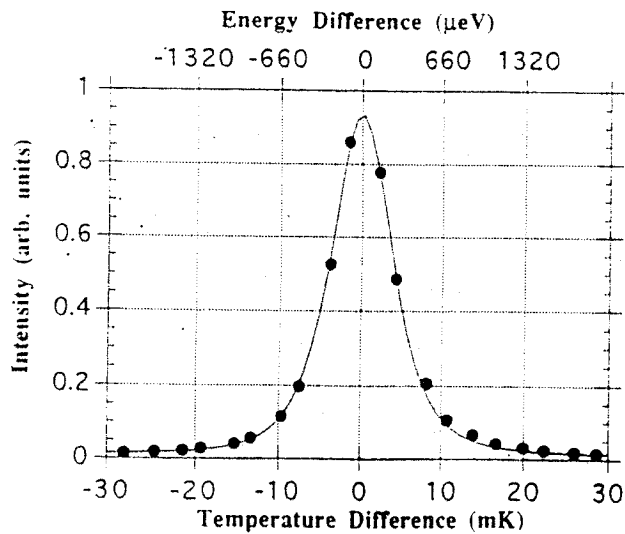
Material (h k l)	$d_H = \frac{4}{2} \lambda_{max}$ (Å)	$r_0 F_H e^{-M/v_0}$ ( $10^{-14}$ cm $^{-2}$ )	Darwin width $\omega_H$ (μrad)	energy resolution $\epsilon_H$ ( $10^{-6}$ )	extinction thickness $t_e$ (μm)	absorption thickness $t_a$ (μm)
Be (002)	1.7916	5.59	10.7	22.8	5.0	1200
Be (110)	1.1428	4.27	6.49	7.1	10.3	1874
C* (111) (diamond)	2.0593	11.1	24.1	59.7	2.20	250
C* (220)	1.2611	9.55	14.9	19.3	4.16	408
Si (111)	3.1354	10.82	34.3	135	1.48	8.7
Si (220)	1.9200	12.29	25.3	57.7	2.12	14.2
Ge (111)	3.2663	23.06	76.0	313	0.66	2.94
Ge (220)	2.0002	27.51	58.5	140	0.91	4.79

most  
commonly  
used

for high  
energies

# SINGLE CRYSTAL PERFECTION

## SILICON



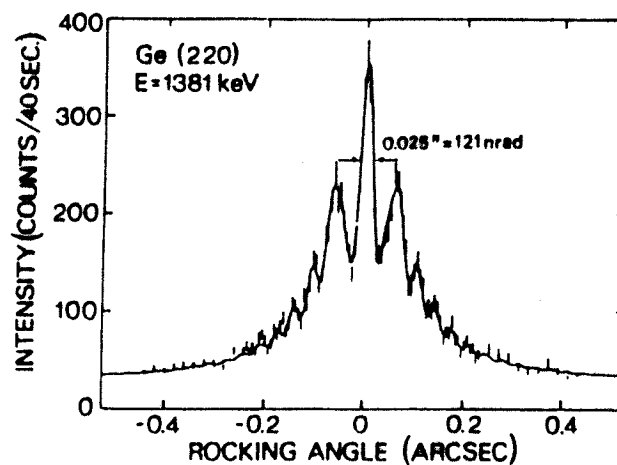
Backscattering Si (13,13,13)  
rocking curve, T-scan at 26 keV

0.5 μeV!     $\Delta E/E = 2 \cdot 10^{-8}$  (FWHM)  $\approx 4 \text{ rad}/d$   
(best value ever achieved)

Sette et al., ESRF Report (1995)

improved to  $\Delta E/E = 9 \cdot 10^{-9} !$

## GERMANIUM



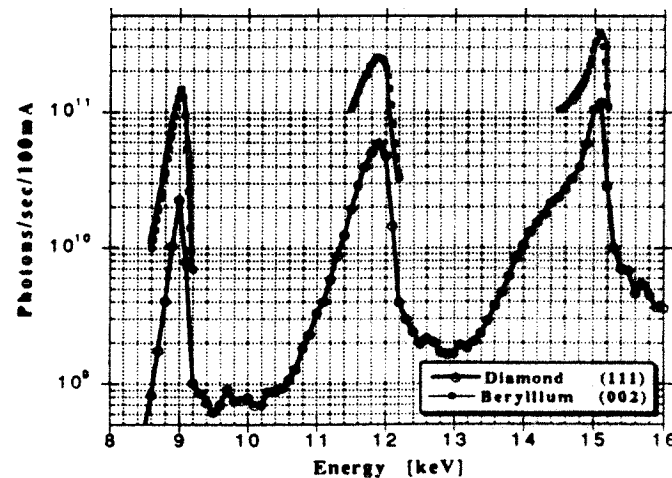
Ge double crystal Laue  
diffraction pattern at 1.4 MeV.

Excess width:  $3 \cdot 10^{-8}$  rad.  
(best value ever achieved)

Freund, RSI 63, 414 ('92)

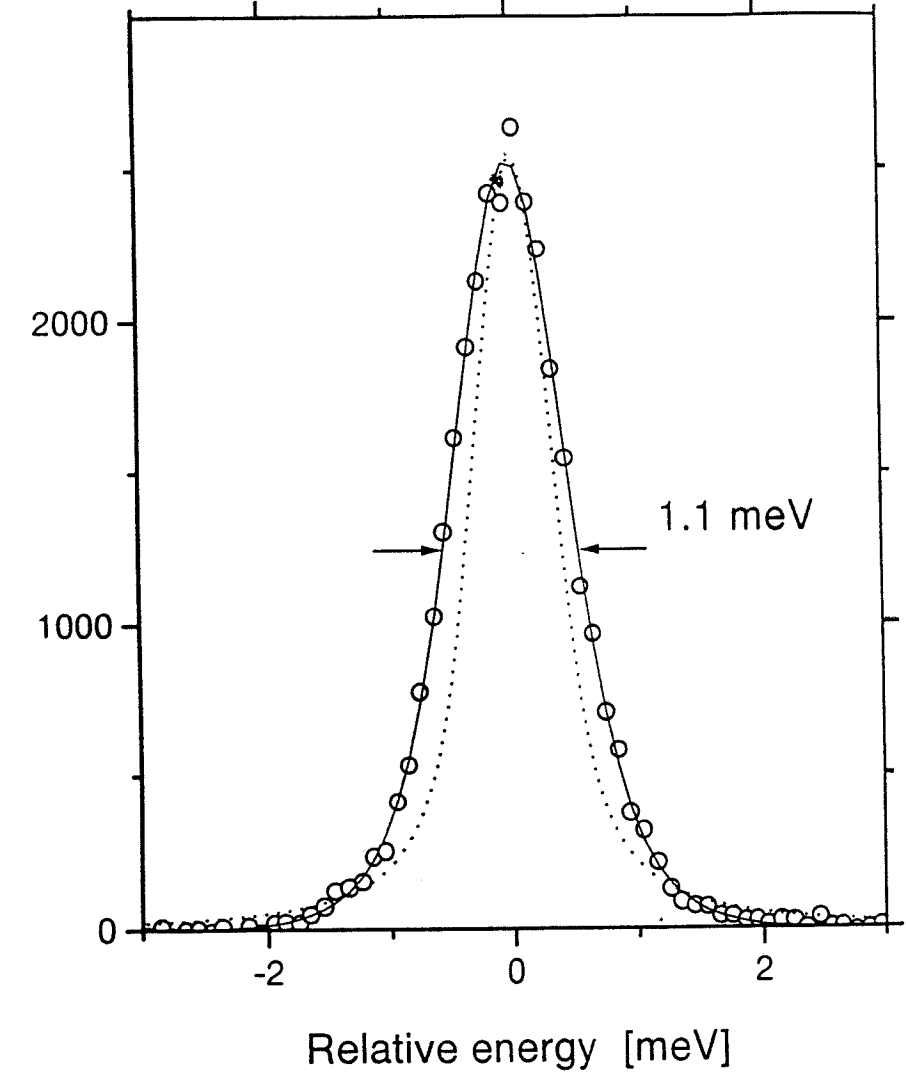
Dewey et al., PR B50, 2800 ('94)

## BERYLLIUM, DIAMOND



ID10 undulator spectra  
recorded with diamond  
and Be single crystals.  
 $0.5 \times 0.5 \text{ mm}^2$  at 44 m.

Grübel et al. J.Phys. C9, 27 ('94)



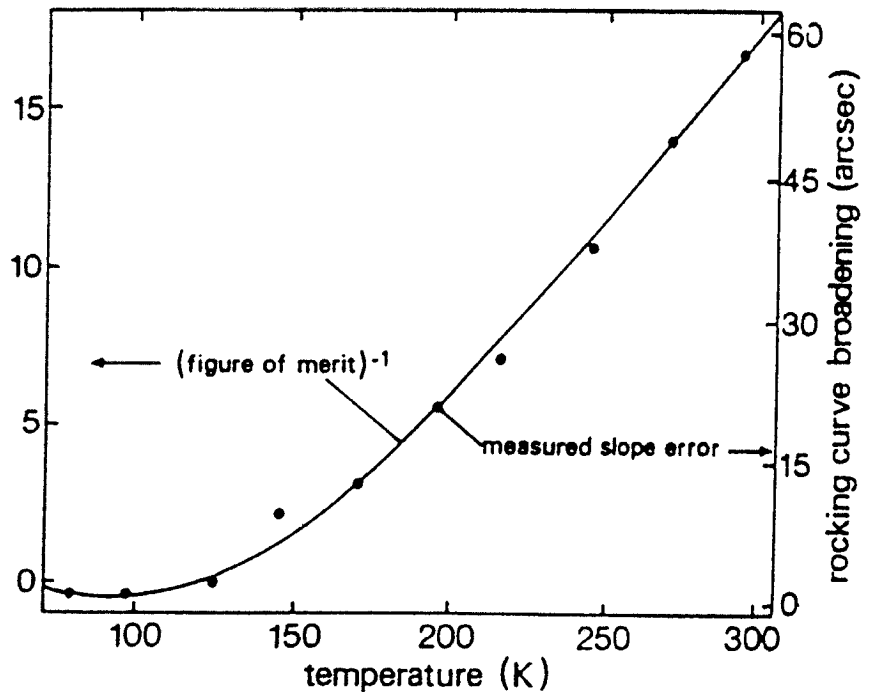
Si (975)  
 $b_1 = 1/20$

Si (975)  
 $b_2 = 20$

Ge (331)  
 $b_0 = 1$

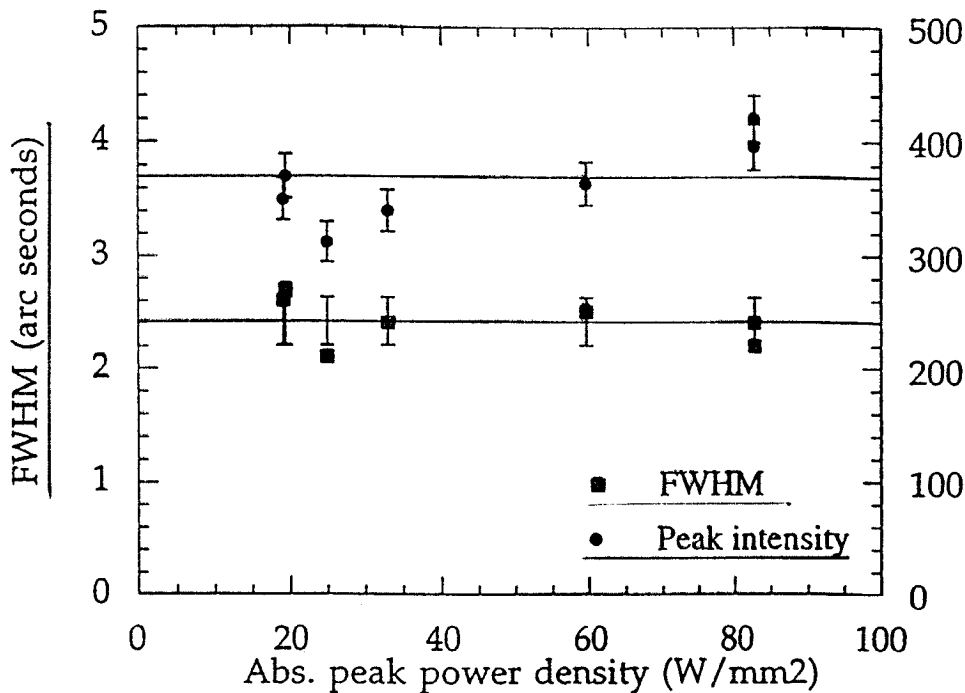
Courtesy: A.CHUMAKOV (ESRF)

# Cryogenic cooling for crystal (and multilayer substrates)



Thick crystal, side cooled  
 $P_s = 150 \text{ W/mm}^2$ ,  $P_t = 80 \text{ W}$   
NSLS X25

A. Freund, Rev Sci. Inst., 63, (1992)  
G. Marot et al. Rev Sci. Inst., 63, (1992)



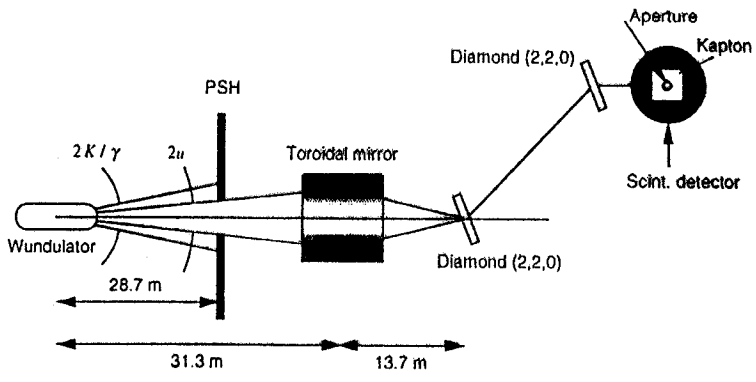
Thin crystal, direct cooled  
 $P_s = 415 \text{ W/mm}^2$ ,  $P_t = 167 \text{ W}$   
ESRF BL3

peak power density  $\approx 20 \text{ kW/mm}^2$   
A. Rogers et al., Rev Sci. Inst., 66, (1995)

# Diamond single crystal - the ultimate



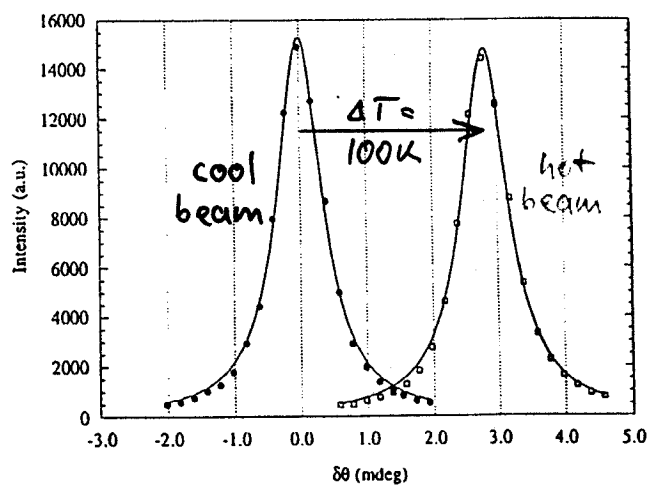
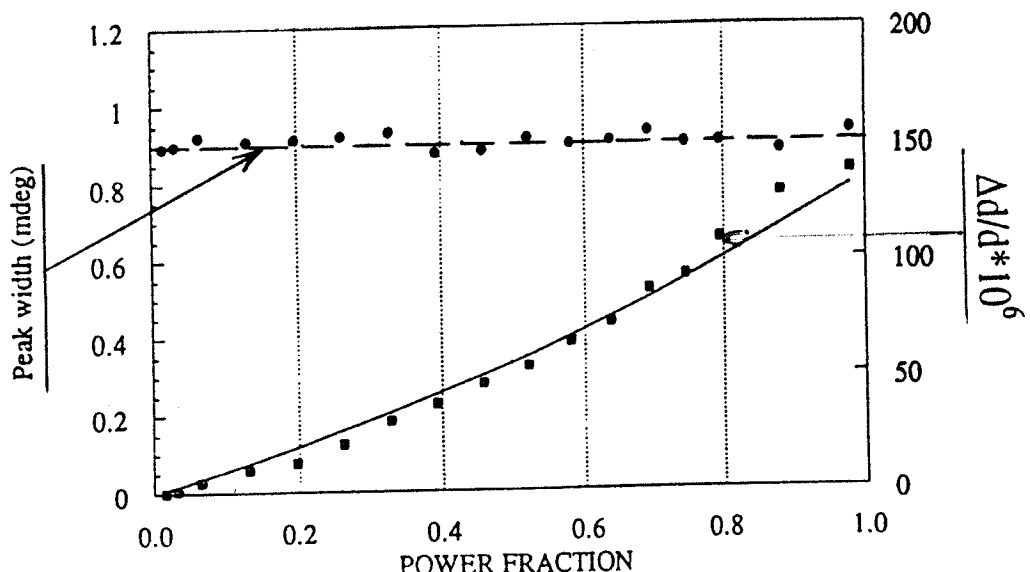
heat load tests @ ESRF on wundulator source BL3/ID9



the beam is focused by the toroidal mirror onto a  $4 \times 8 \times 0.1 \text{ mm}^3$  synthetic diamond crystal (Laue case)  
 (supplied by F. Sellschop, University of Johannesburg)

- incident [spot  $0.2(h) \times 0.4(v) \text{ mm}^2$ ]:  $P_t = 280\text{W}$   $\Rightarrow P_s = 3500\text{W/mm}^2$
- absorbed :  $P_t = 8.7\text{W}$  (3.1%) and  $P_s = 109\text{W/mm}^2$

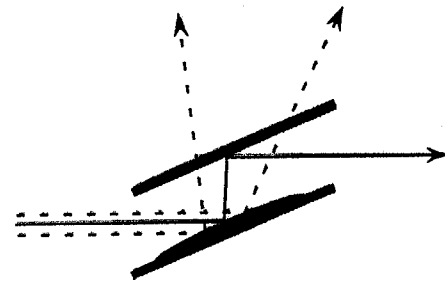
Heat flux  $86 \times$  that on  
 the sun's surface!!!



# Heat Problem : Crystal case



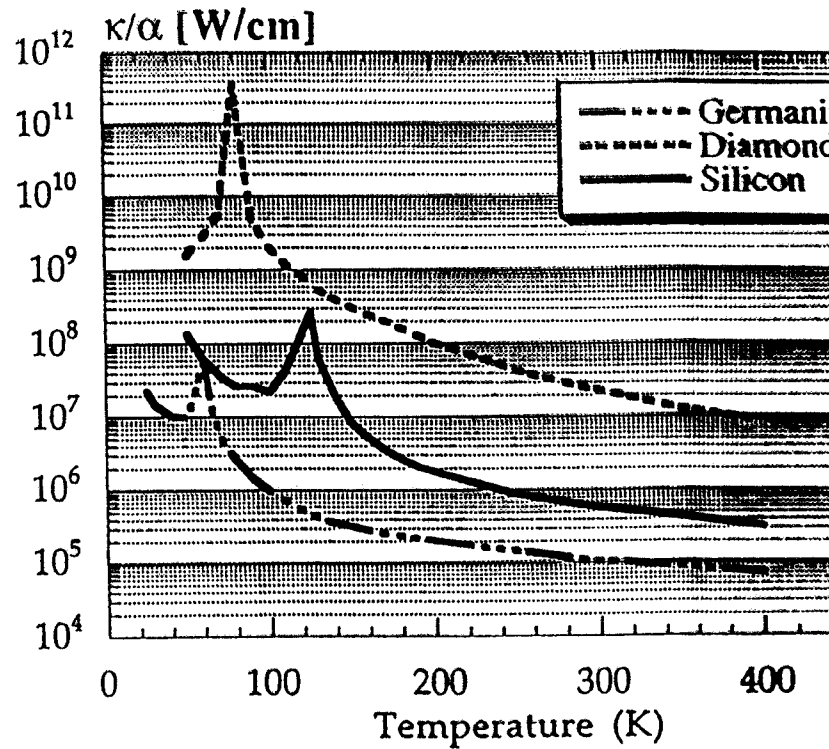
- usually  $P_s$  very high  $\Rightarrow \Delta_{\text{bump}} > \Delta_{\text{bending}}$  : for undulator radiation.



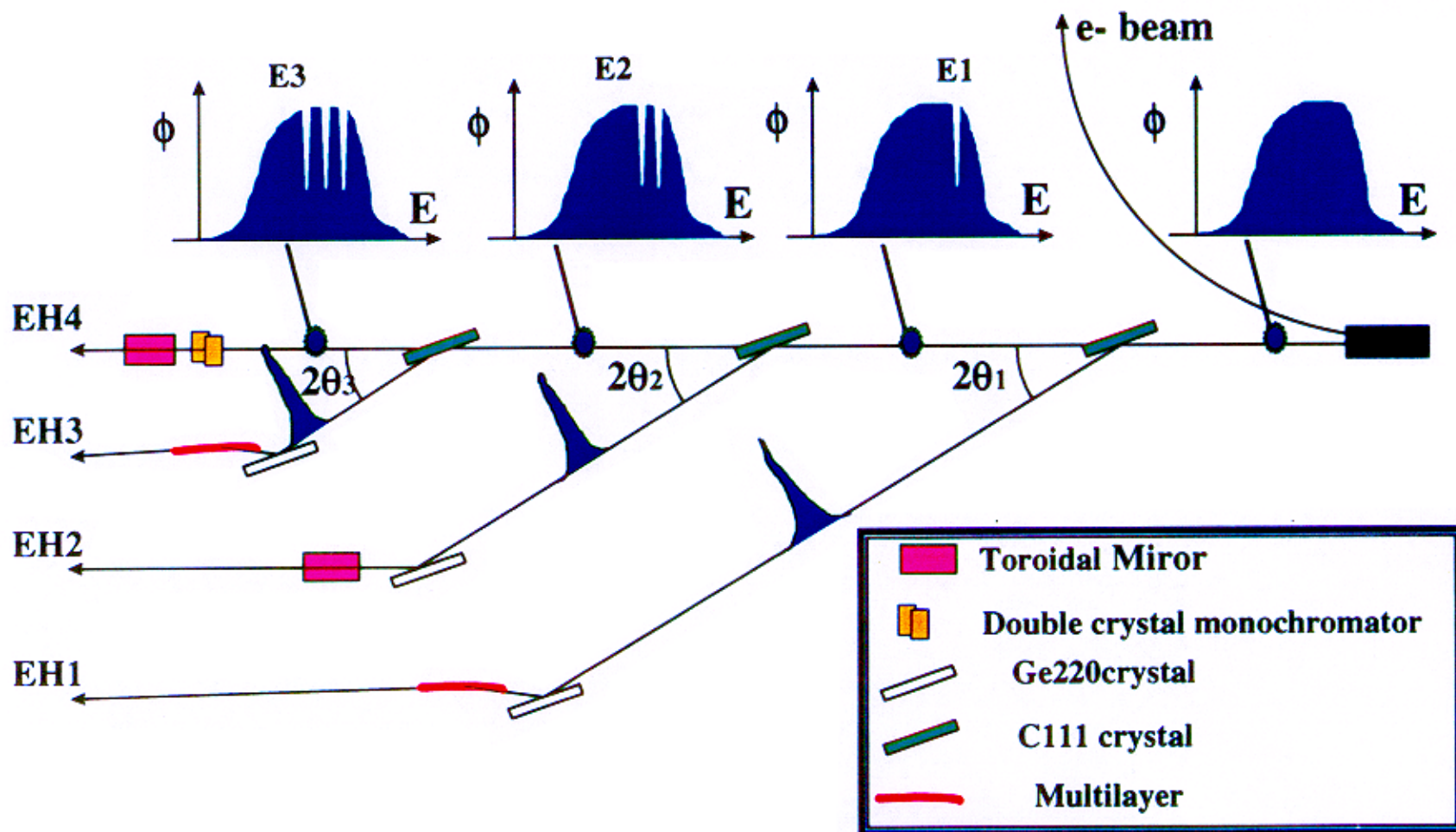
- one reflection : increase of beam divergence and bandpass
- double reflection : loss of transmission

Material	Be	C*	Si	Ge
Crystal	hcp	diamond	diamond	diamond
$\mu @ 8\text{keV} [\text{cm}^{-1}]$	$1.8 \text{ cm}^{-1}$	$1.8 \text{ cm}^{-1}$	$7.5 \text{ cm}^{-1}$	$141 \text{ cm}^{-1}$
$\kappa @ 297\text{K} [\text{Wcm}^{-1}\text{K}^{-1}]$	1.94	23	1.5	0.64
$\alpha @ 297\text{K} [10^{-6} \text{ K}^{-1}]$	7.7	1.1	2.4	5.6
$\kappa/\mu\alpha @ 297\text{K} [\text{MK}]$	0.14	2.80	$5 \cdot 10^{-3}$	$3 \cdot 10^{-4}$
@ 77K [MK]	11	120	$2 \cdot 10^{-1}$	$7 \cdot 10^{-3}$

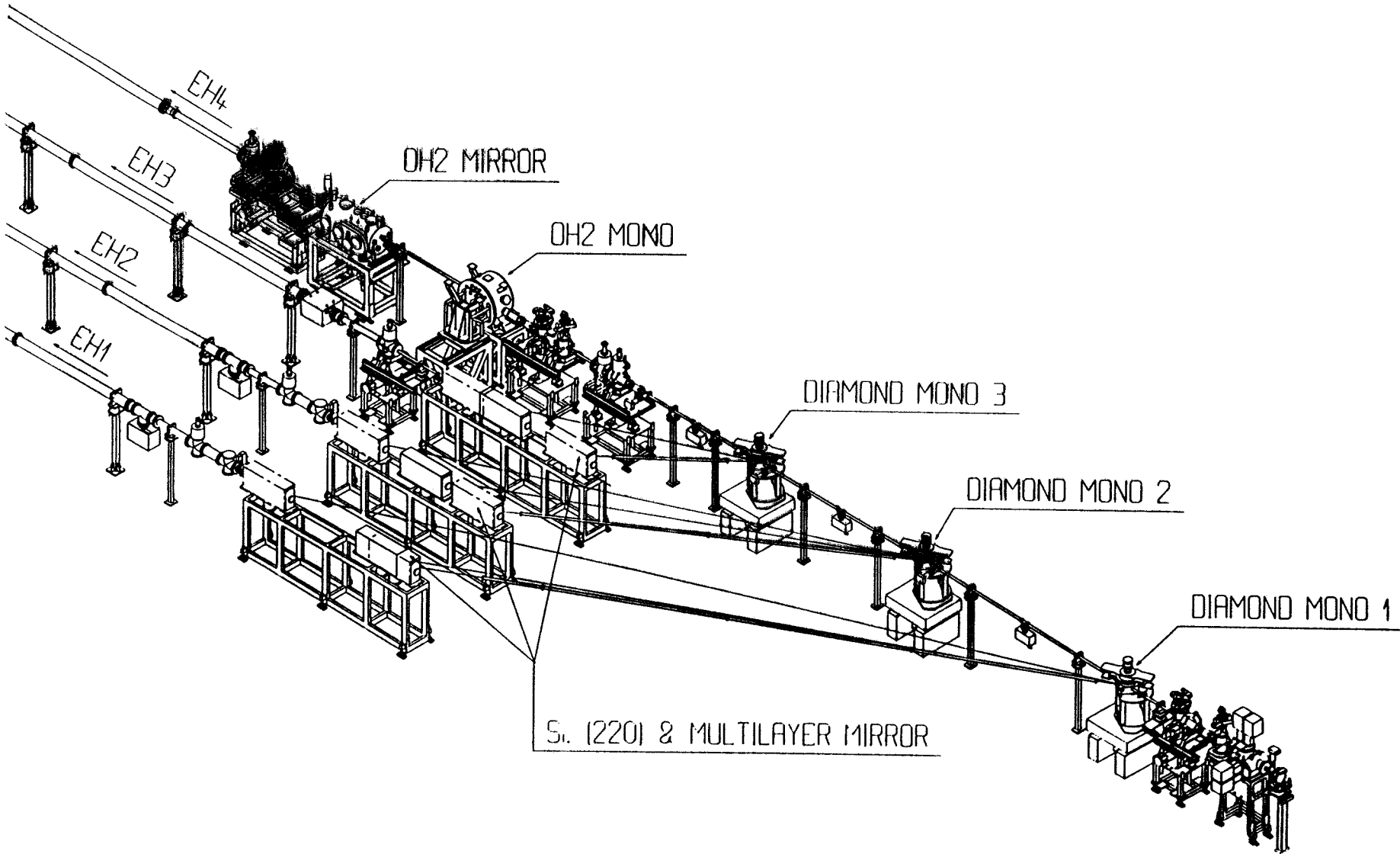
$$\Delta_{\text{bump}} \propto \frac{\alpha}{K} G P e^{-\mu x} \begin{cases} \mu x < 1 \Rightarrow x = t \\ \mu x > 1 \Rightarrow x = t_{\text{abs}} \end{cases}$$



# ID14-Quadriga principle



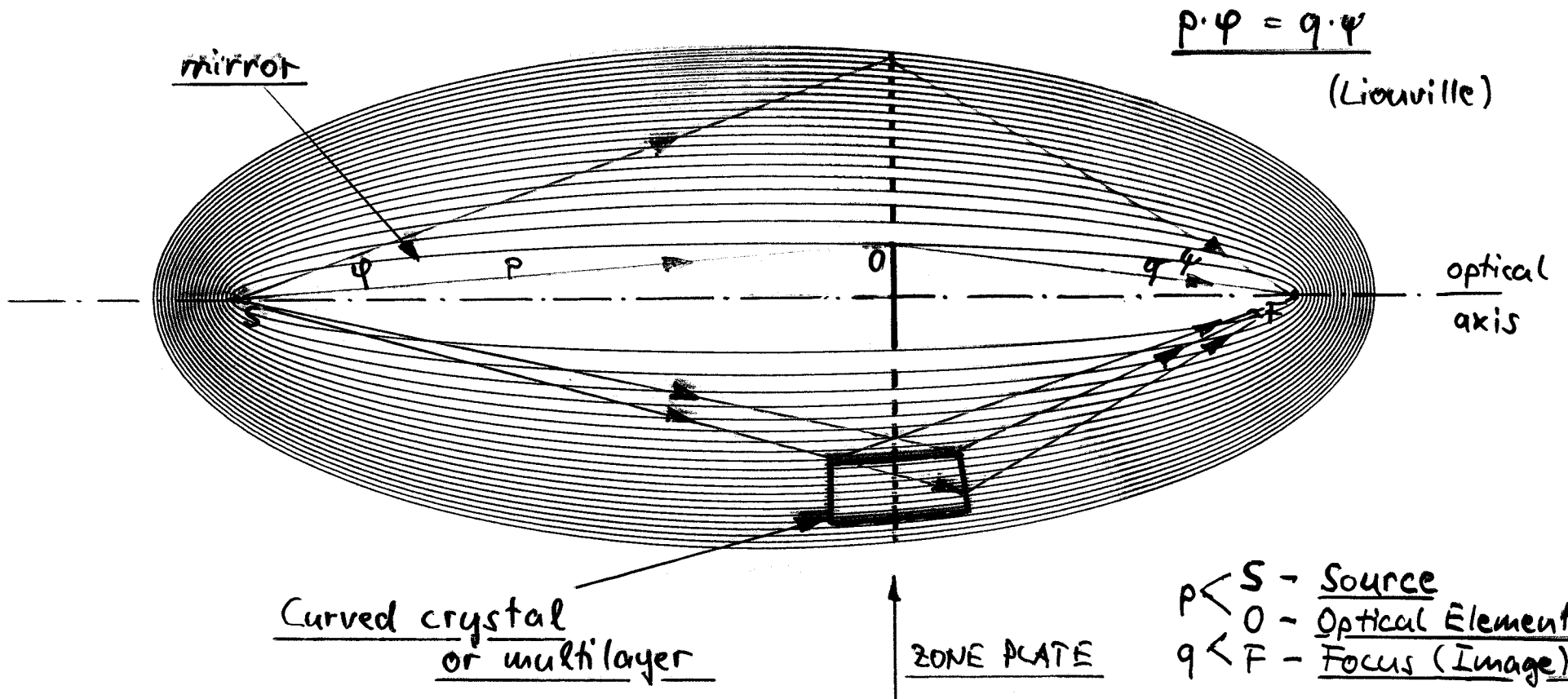
Courtesy: S.WAKATSUKI (ESRF)



Courtesy: S. WAKATSUKI (ESRF)

# FOCUSING

⇒ All imaging elements can be seen as sections of holograms of a point with a spherical reference wave.



⇒ The isophase figures are confocal ellipses  
(see also: Spiller! "Soft X-ray Optics", SPIE, 1994)

$$p \cdot \psi = q \cdot \psi$$

(Liouville)

optical  
axis

Curved crystal  
or multilayer

ZONE PLATE

$p < S$  - Source  
 $O$  - Optical Element  
 $q < F$  - Focus (Image)

$$M = q/p = \psi/\psi$$

(Magnification)

# FOCUSING OPTICS FOR HARD X-RAYS

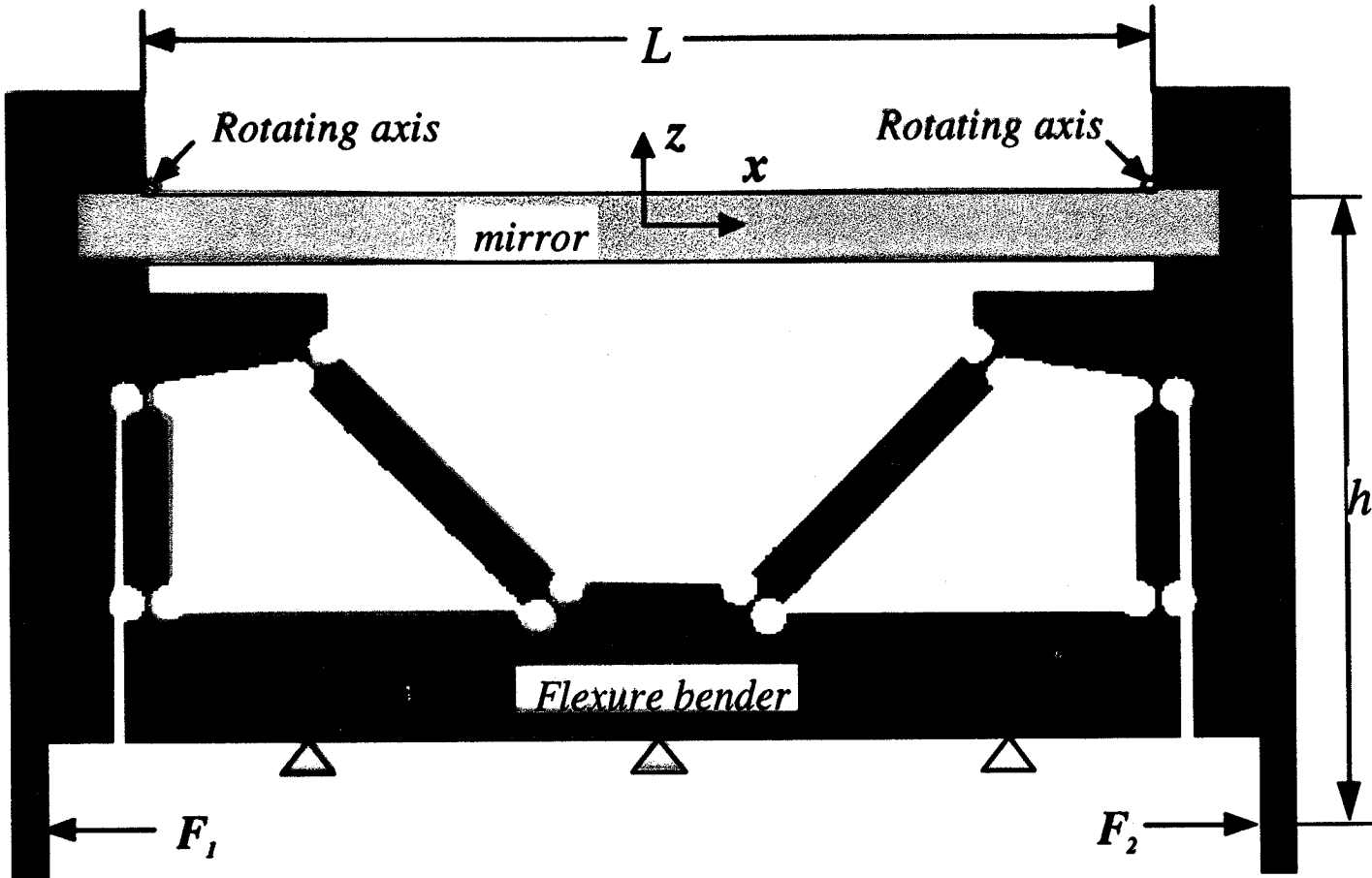
$3 \text{ keV} < E < 100 \text{ keV}$

---

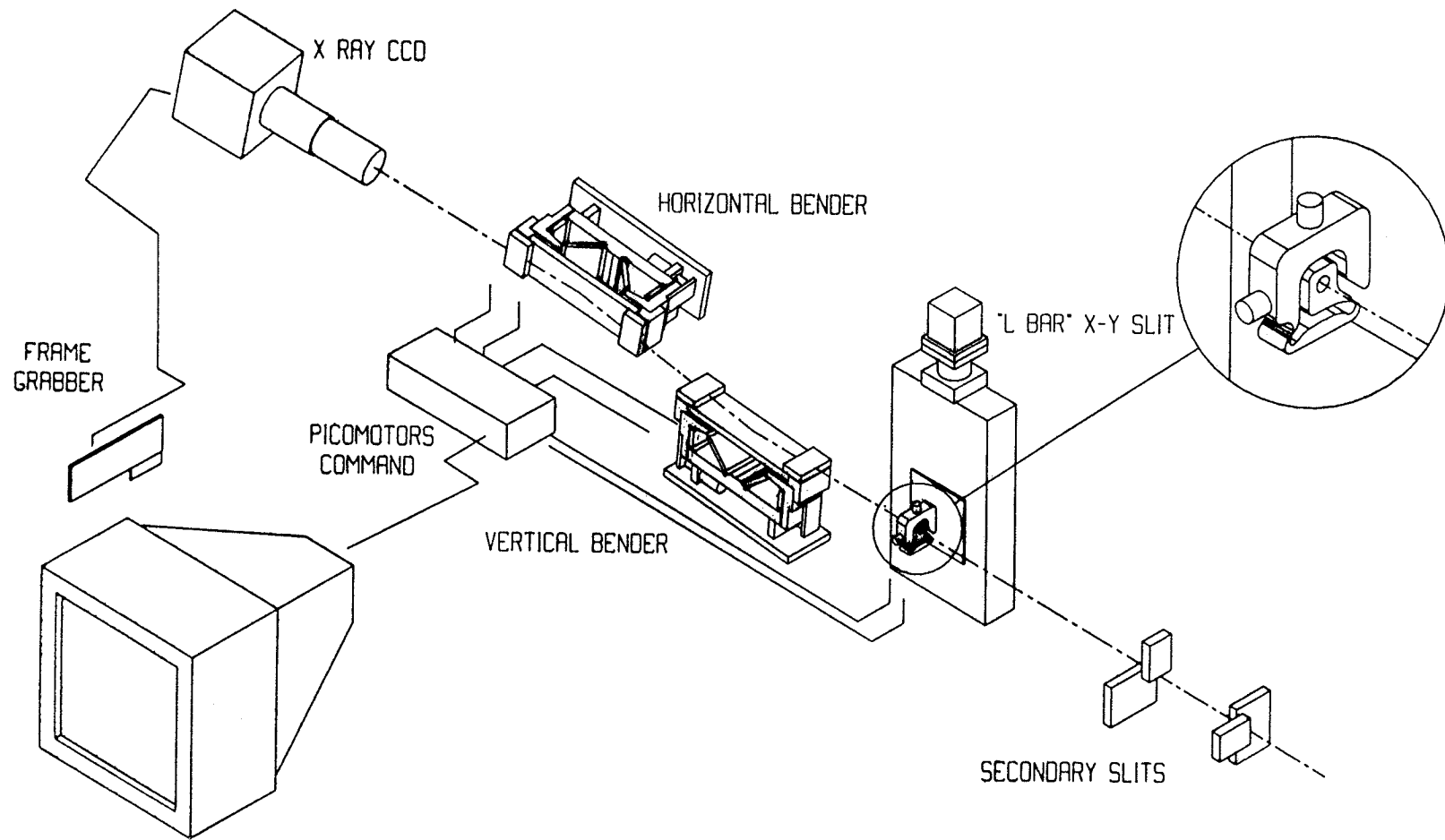
(after Snigirev, 1995)

	KINEMATICAL FOCUSING BENT MIRROR OR CRYSTAL			DYNAMICAL FOCUSING			CAPILLARY OPTICS	FRESNEL OPTICS	BRAGG- FRESNEL OPTICS
		Indenbom 1974	Afanas'ev,Kohn 1977	Petrashen', Chukhovsky 1976	Kreger 1948	Baez 1952	Aristov et al 1986		
	mirror Kirkpatrick, Baez 1948	multilayer Underwood, Barbee,Frieber 1986	crystal Johann, Johansson 1931-1933						
angular aperture	$10^{-3}$	$10^{-3}$	$10^{-4}$	$10^{-4} - 10^{-5}$			$10^{-3}$		
resolution	$5\mu\text{m}$ Suzuki et al 1992	$5\mu\text{m}$ Underwood et al 1988	$10\mu\text{m}$ Van Lagevelde 1992	$<10\mu\text{m}$			0.05 Bilderback et al 1994	0.6 $\mu\text{m}$ Yun et al 1992	0.5-0.7 Snigirev et al 1994-95

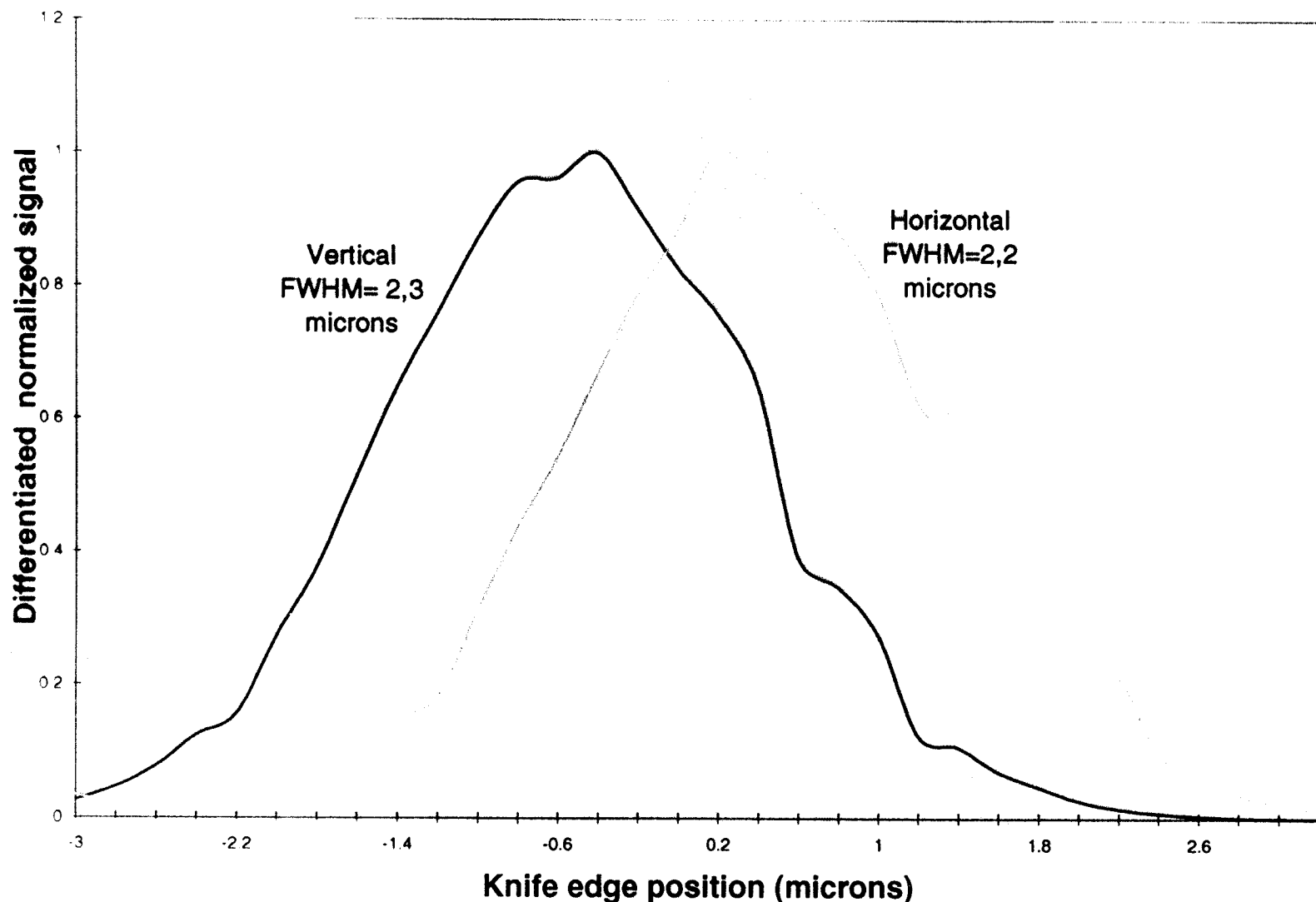
## Finite element model of the flexural hinge-based bender



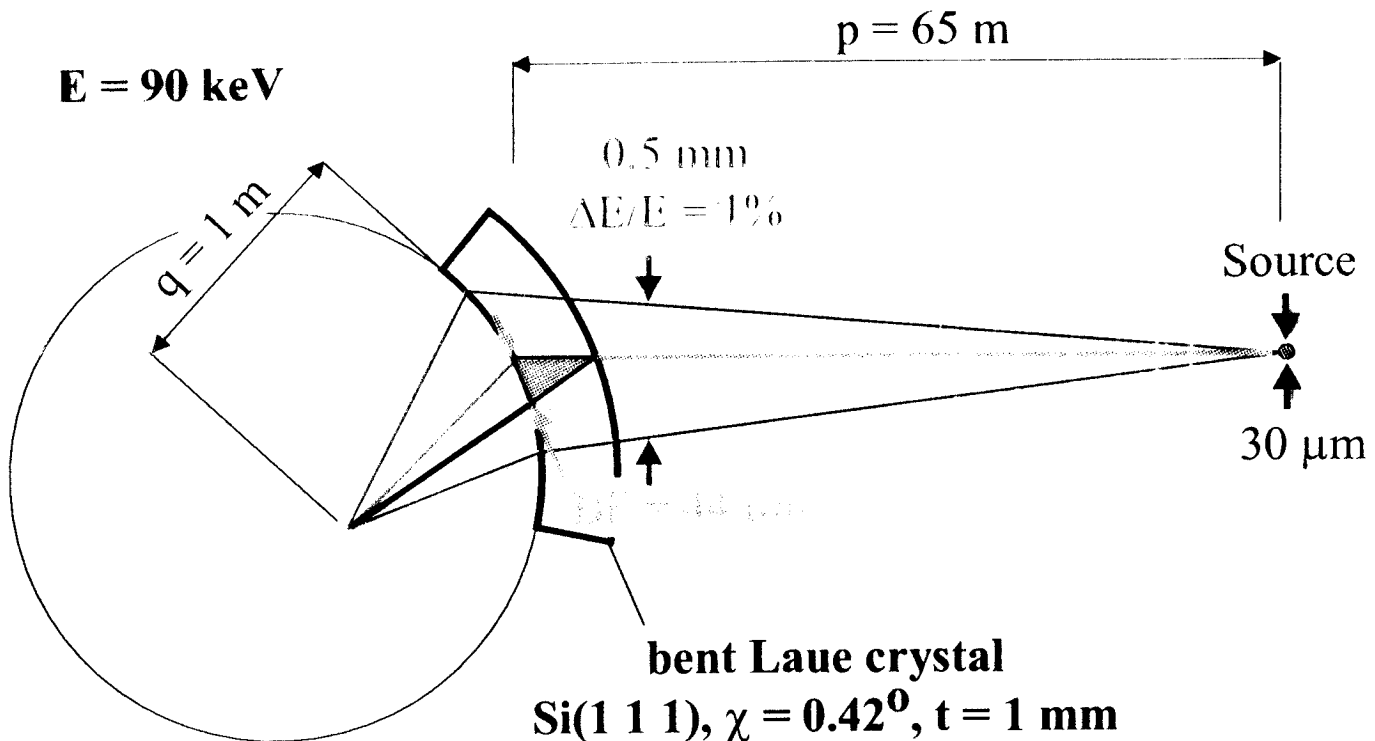
the piezo actuators are illustrated by 2 arrows  
the triangles  $\Delta$  represent fixations

**KIRPATRICK BAEZ AUTOMATED SHAPING**

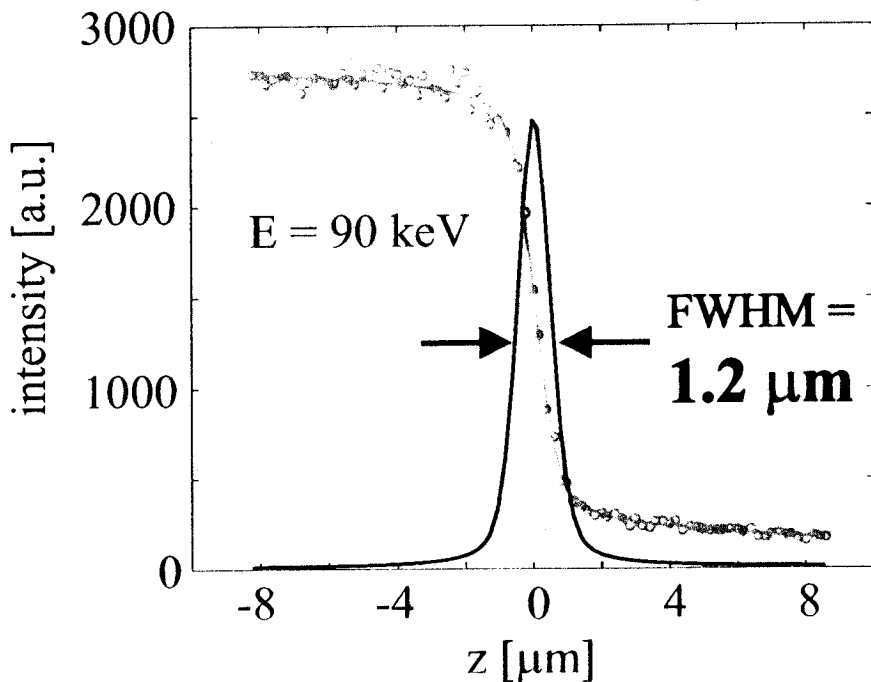
Bidirectional focusing on BM5 E = 9 KeV 800X800 microns Gain #10<sup>5</sup>



# Laue focusing

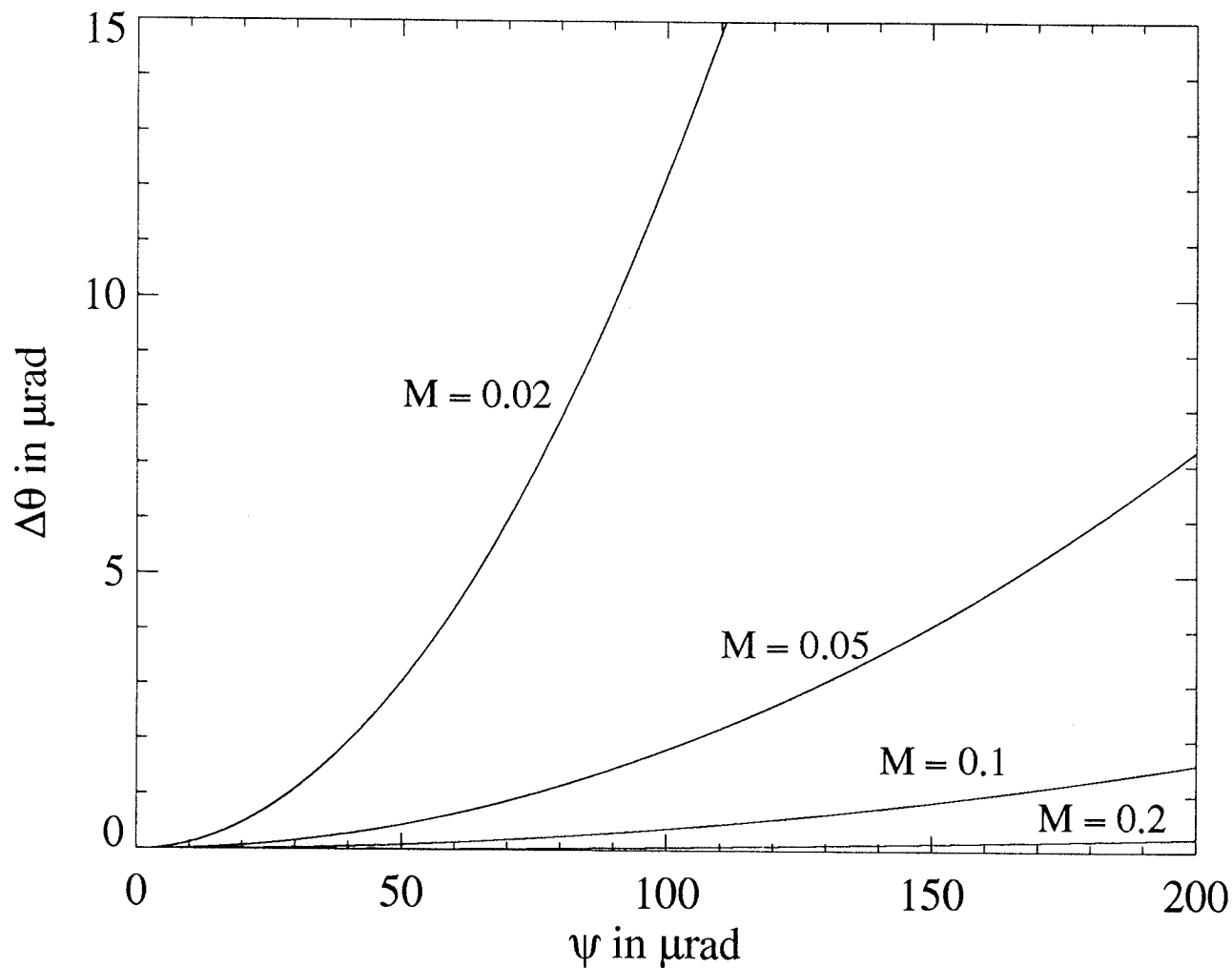


## Fluorescence knife-edge scan

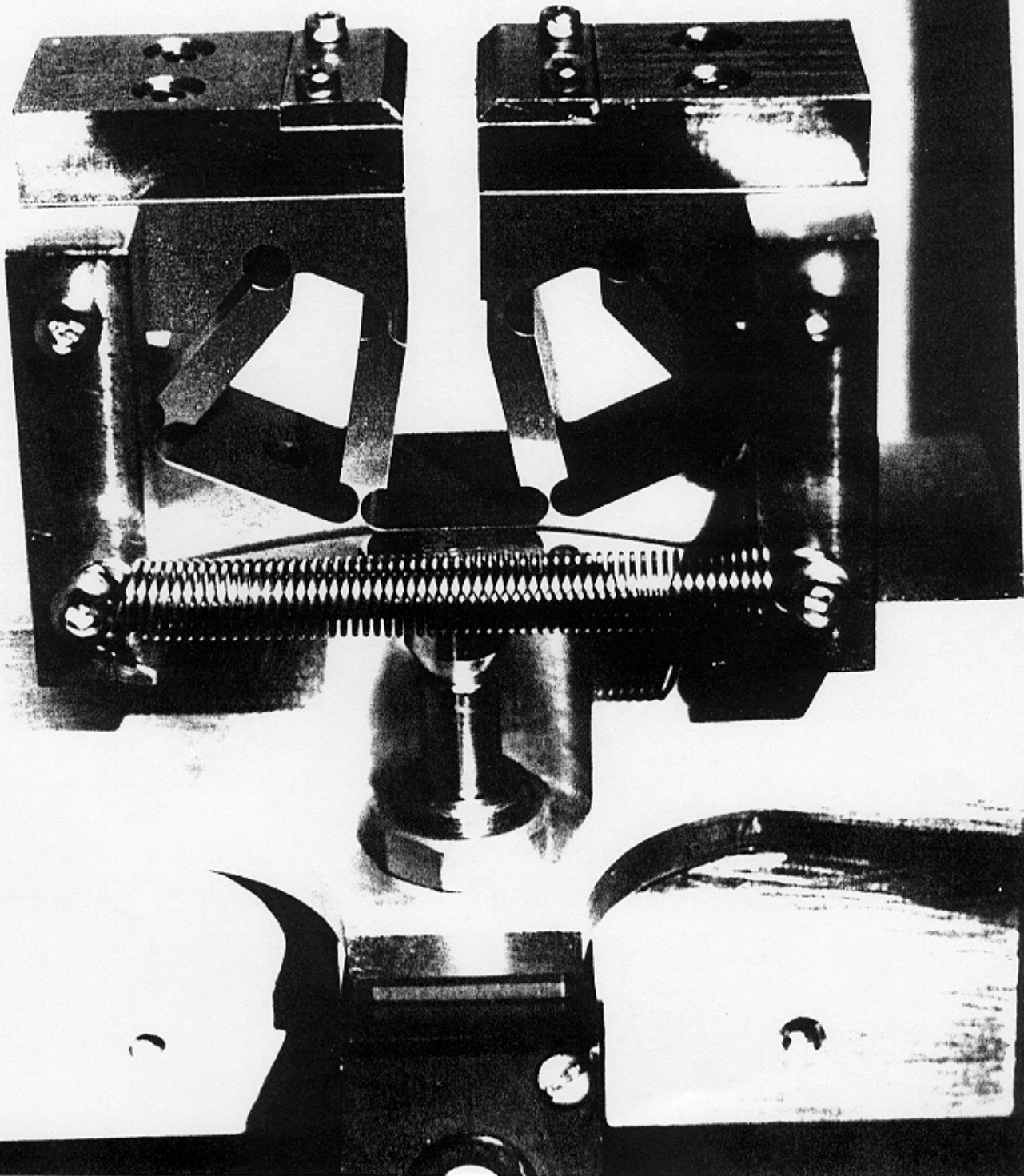


- flux in  $1.2 \times 500 \mu\text{m}^2$ :  
 $4.3 \cdot 10^9 \text{ ph/s/0.1 \AA}$
- efficiency: 90 %
- gain factor: 300

$$\Delta\theta = \frac{\psi^2(1+M)(3M-1)}{8M^2\sin\theta_B}$$

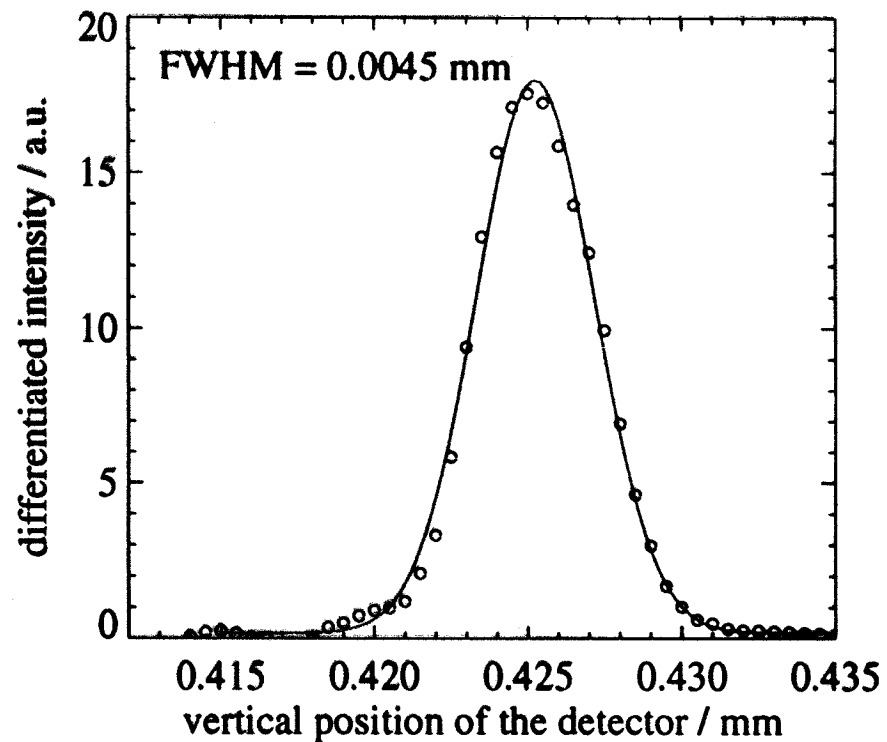
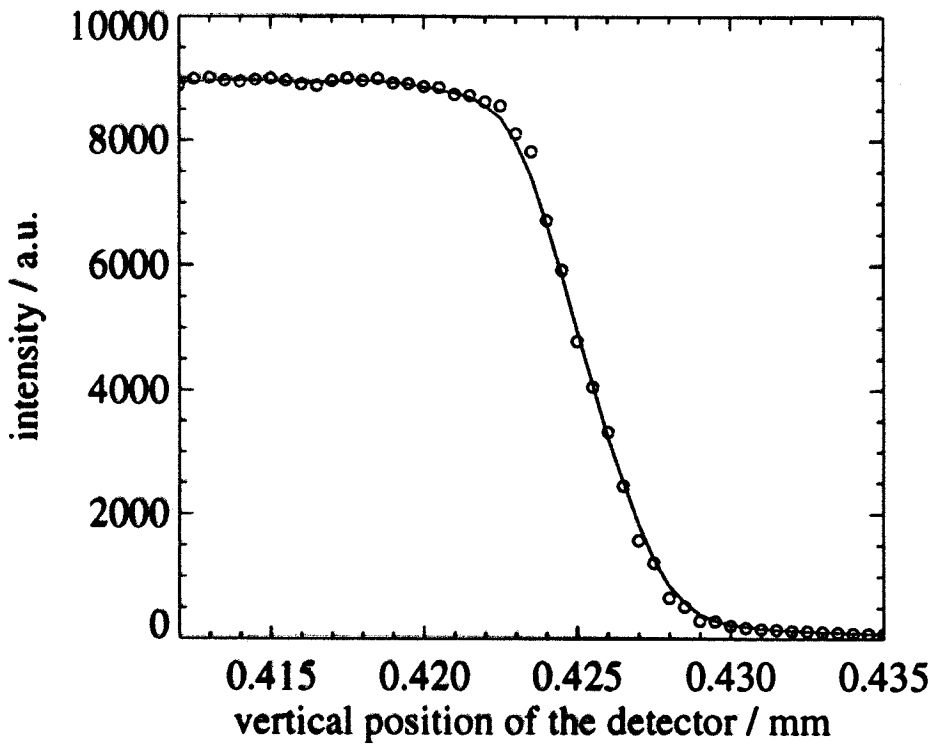


Angular errors in dependence of the divergence  $\psi$ , for different magnifications. Calculated for Si(111) and an energy of 8047.8 eV.



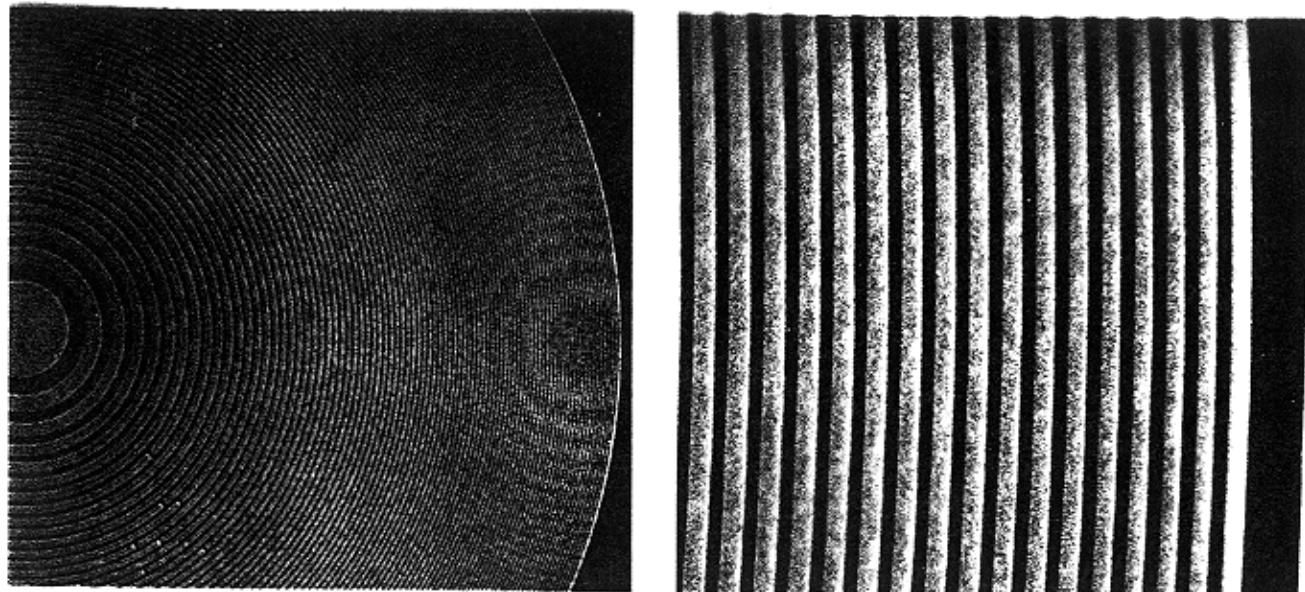
# Focal spot, produced by a bent silicon[111] crystal

Knife edge scan; Energy = 8.047 keV



# FZP

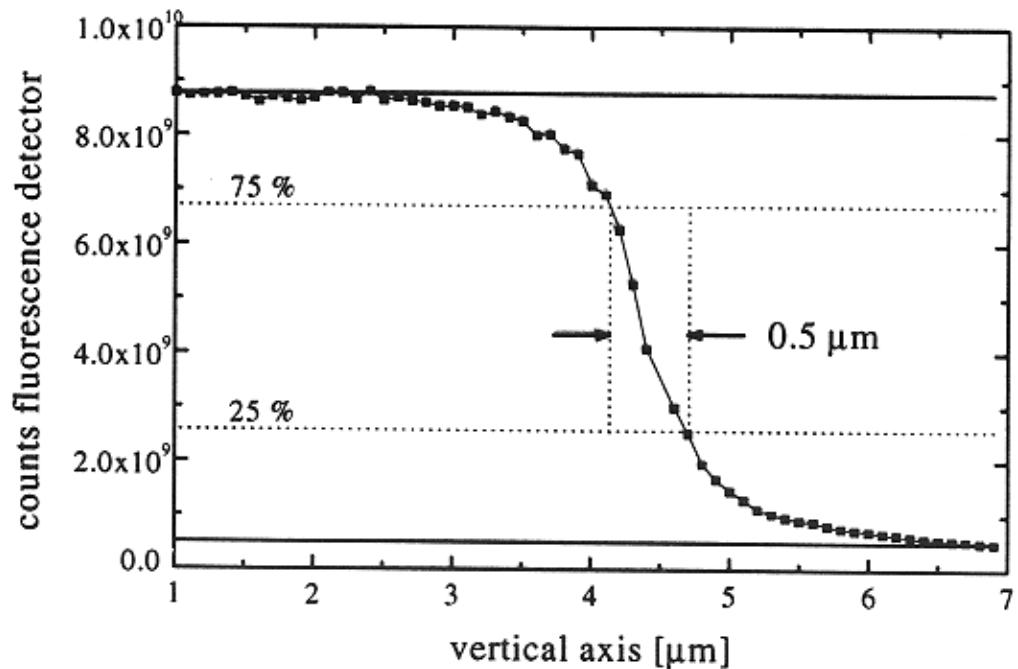
E.Di Fabrizio,  
M. Gentili,  
*IESS, CNR, Rome, Italy*



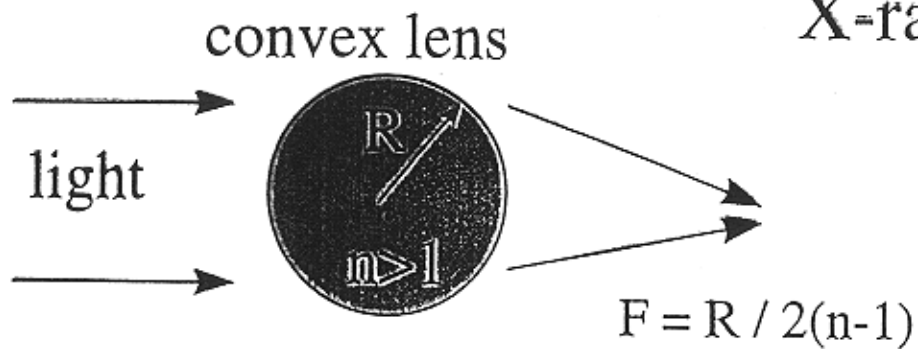
Cr-mask scan to resolve the spot size:  $0.5 \mu\text{m}$  (V),  $6 \mu\text{m}$  (H), flux  $10^{10} \text{ ph/s}$

## Fresnel zone plate parameters

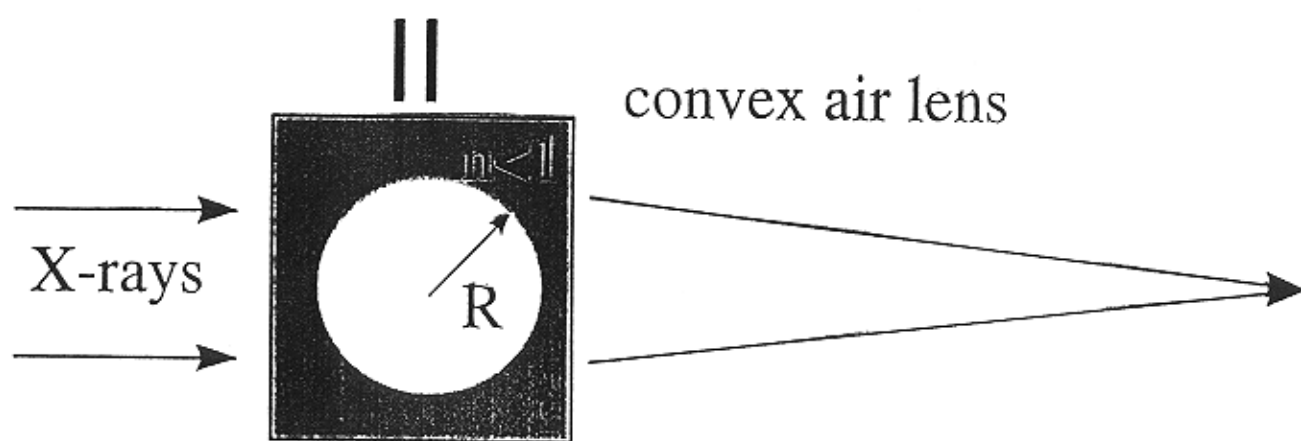
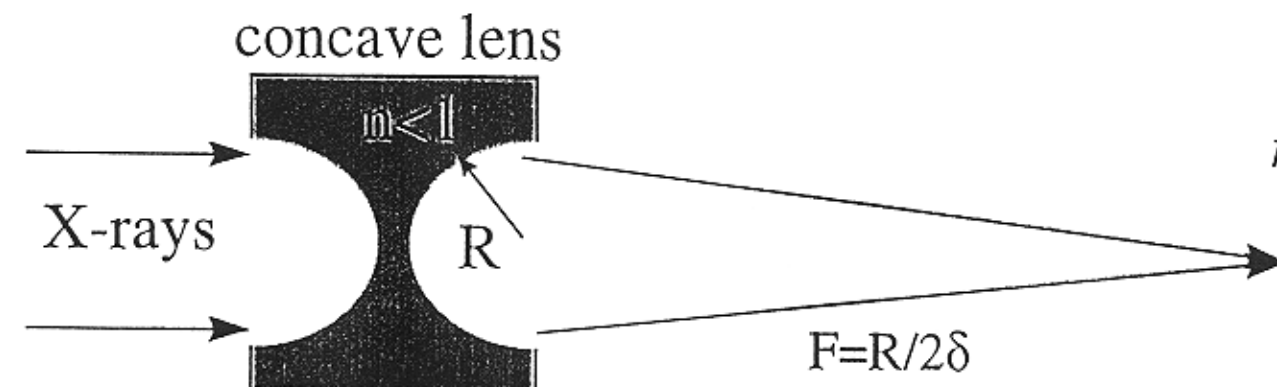
169 zones, radius first zone:  $7.8 \mu\text{m}$   
radius last zone:  $0.3 \mu\text{m}$   
zone material: gold, thickness:  $1.15 \mu\text{m}$   
substrate: SiN, thickness:  $2 \mu\text{m}$   
aperture:  $200 \mu\text{m}$   
focal length 8 keV: 400 mm  
12 keV: 600 mm



# X-rays versus Light



$$n > 1 \quad n-1 \sim 0.1$$



Be

$E = 10 \text{ keV}$

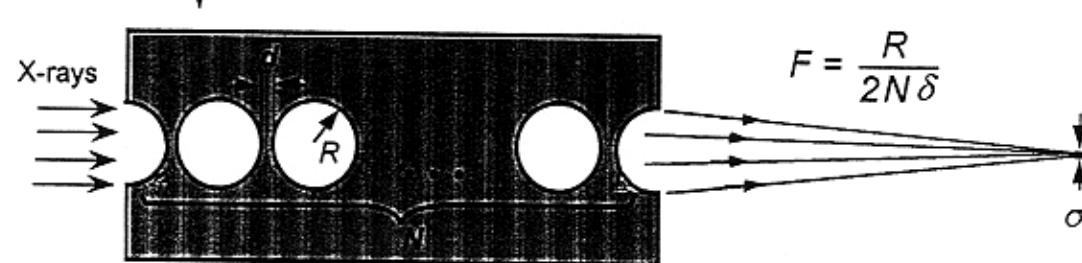
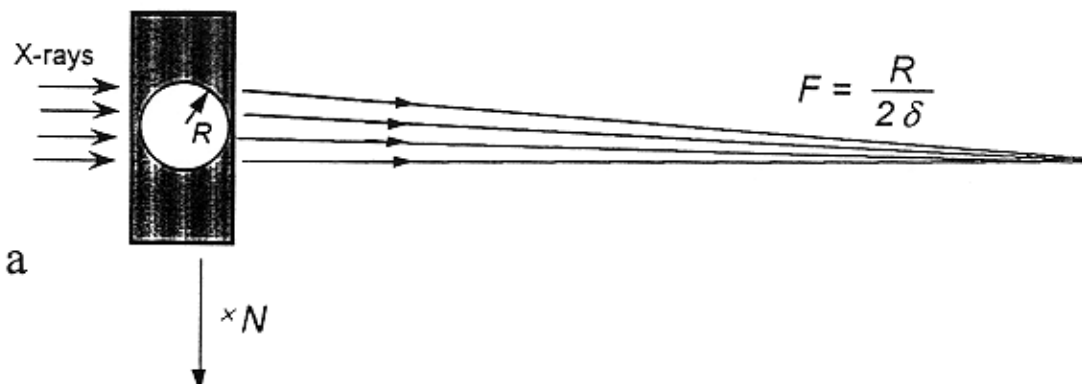
$\delta = 3.4 \cdot 10^{-6}$

$R = 100 \mu\text{m}$

$F = 15 \text{ m}$

# Compound Refractive Lens

Snigirev A., Kohn V., Snigireva I., Lengeler B., *Nature*, November 7, 1996



b

resolution

$$\sigma_f = \frac{\lambda r_f}{A},$$

effective aperture is limited by spherical aberrations or by absorption

$$A_t = 2R \left( 4 \frac{\lambda r_f}{R^2} \right)^{\frac{1}{4}},$$

$$A_a = 2R \left( \frac{2}{\mu R N} \right)^{\frac{1}{2}},$$

real gain  $g = a G \frac{\sigma_f}{\sigma_1} = a \frac{A}{\sigma_0} \left( \frac{r_0}{r_f} + 1 \right)$ , where  $a = \exp(-\mu Nd)$ ,  $\sigma_1 = \sigma_0 r_f / r_0$

chromatic aberrations

$$\frac{\Delta\lambda}{\lambda} \approx \frac{\beta}{\delta}$$

index of refraction

$$n = 1 - \delta + i\beta < 1 \quad (\delta > 0),$$

X-ray collecting lens has a **concave shape**

$$\text{for Al at } E = 10 \text{ keV} \quad \delta = 0.55 \cdot 10^{-5}$$

$$1 \text{ hole of } 100 \mu\text{m radius} - \quad F = 9 \text{ m}$$

$$15 \text{ holes of } 100 \mu\text{m radius} - \quad F = 60 \text{ cm}$$

$$\text{Gaussian lens formula: } r_f = F \left( 1 - \frac{F}{r_0} \right)^{-1}$$

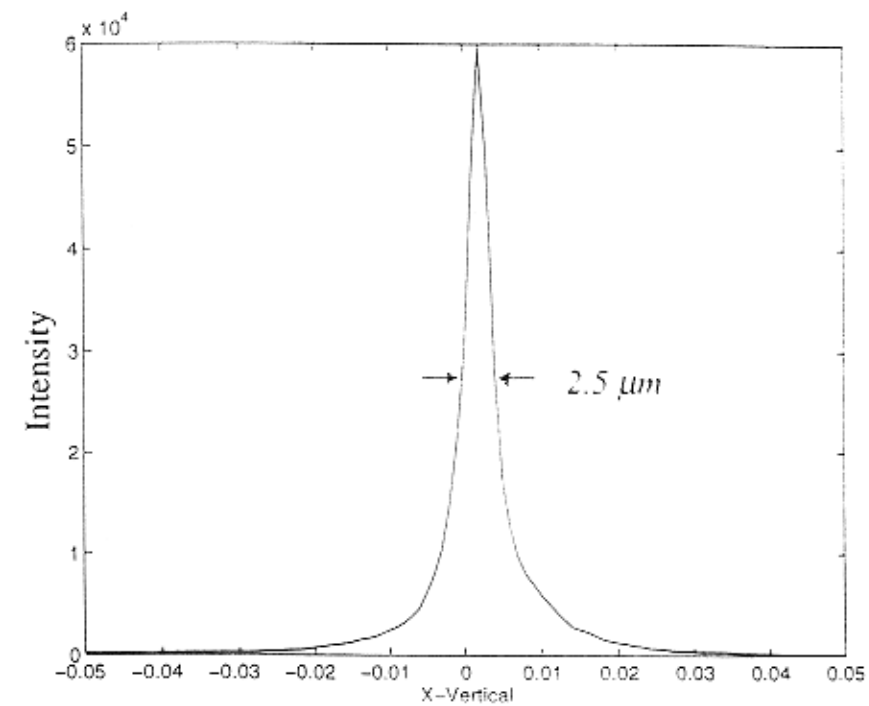
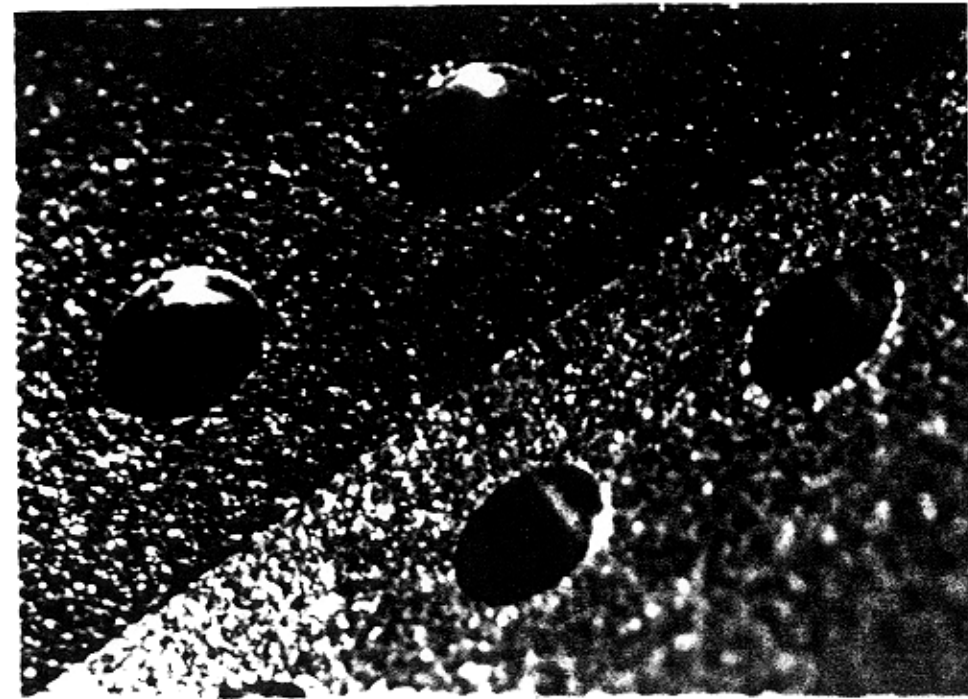
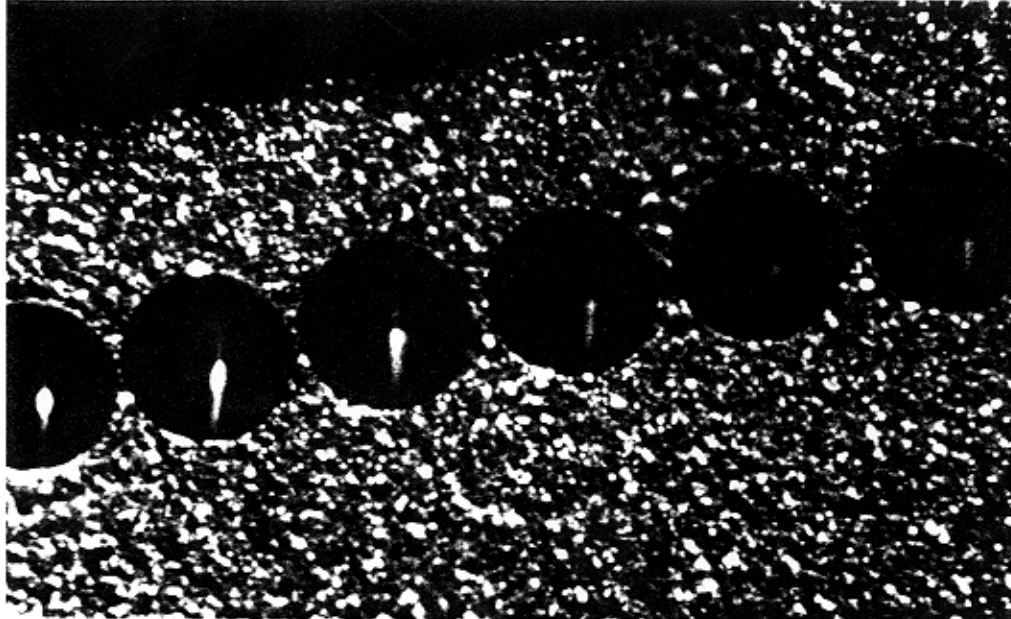


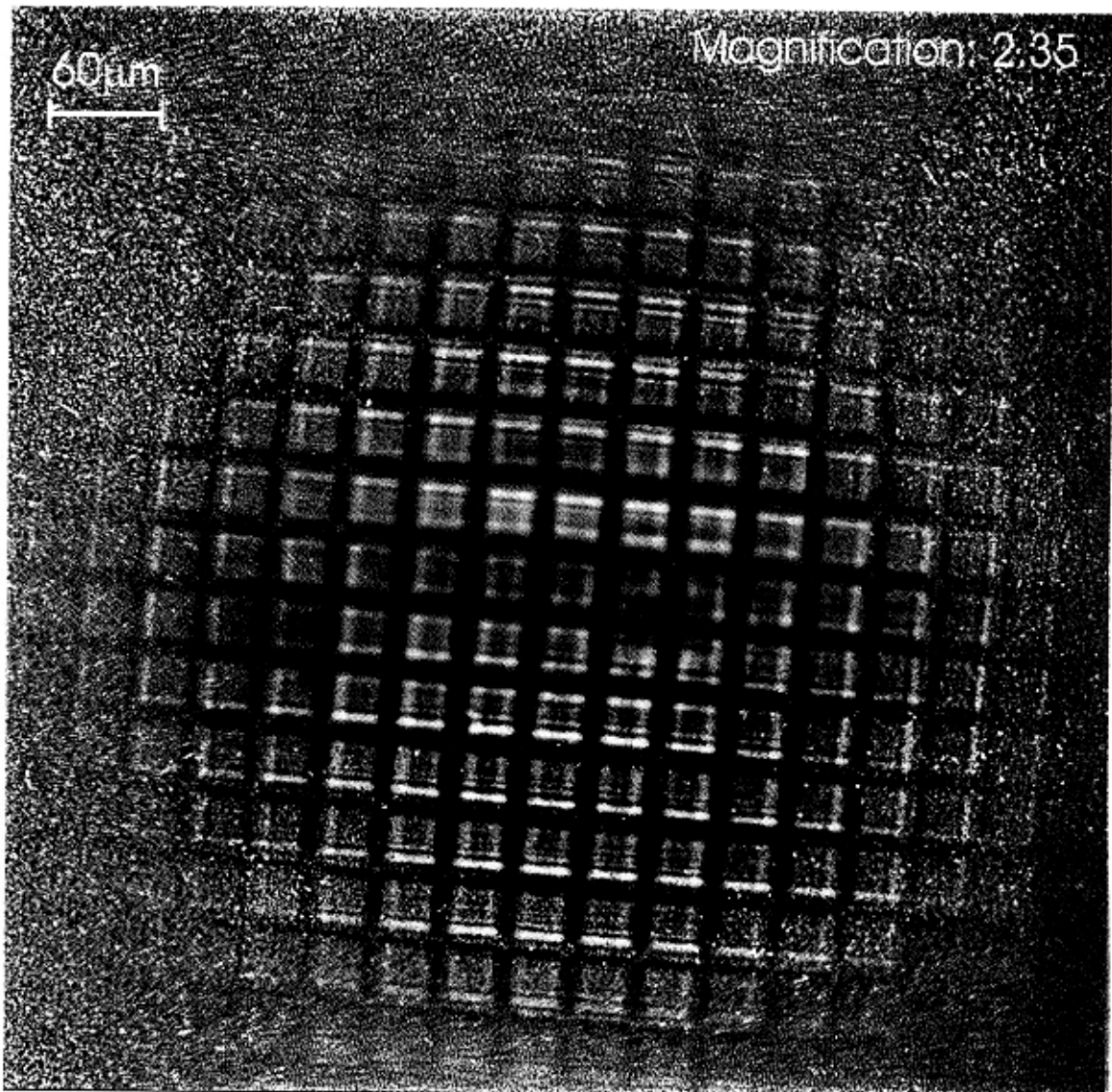
Image in optical microscope of linear and two-dimensional Be CRLs with 69 holes of 500  $\mu\text{m}$  diameter. Spacing in the thinner part between holes is about 100  $\mu\text{m}$ .

Intensity distribution of the focal spot at 0.9 m focal distance for Be CRL at 9 keV X-ray energy. Width of the focusing line was measured of about 2.5  $\mu\text{m}$  and was limited by the source size.

## *Optical properties of cylindrical CRLs. Experimental results.*

Material	Hole radius, <i>R</i> (mm)	Distance between the holes, <i>d</i> ( $\mu\text{m}$ )	Energy, <i>E</i> keV	Focal length, <i>F</i> (m)	Number of holes, <i>N</i>	Spot size (FWHM), (vert./hor.) $\Delta$ ( $\mu\text{m}$ )	Gain, <i>g</i>
<i>Be</i>	0.50	100	12.6	1.7	69	3.4	5.7
<i>Be</i>	0.50	100	9.0	0.87	60	2.6	2.0
<i>Be</i>	0.25	20	12.5	1.09	53	3.3	9.0
<i>Be crossed</i>	0.50	50	9.2	1.82	36.5/37	7.6/19	13.6
<i>Boron Nitride</i>	0.25	50	12.5	1.64	39	-	-
<i>Pyrocarbon</i>	0.35	39	16.4	1.70	59	4.2	12.6
<i>Teflon</i>	0.35	38	23.7	1.78	134	11.0	1.0
<i>Teflon crossed</i>	0.35	38	16.7	1.83	67/67	5.2/18	0.8
<i>PMMA</i>	0.25	30	12.5	1.27	59	10.0	4.5
<i>Polycarbonate</i>	0.25	50	12.5	1.88	40	4.9	6.5
<i>Polyoxymethylene</i>	0.25	30	12.5	1.61	40	3.5	4.4
<i>Vespel</i>	0.25	30	12.5	1.28	50	5.0	1.9
<i>Al (0.5%Mg))</i>	0.50	38	18.8	1.70	96	3.5	1.3
<i>Al(2x)</i>	0.50	38/40	27.1	1.70	192	4.5	1.3

# Imaging of a gold grid (15 µm period) by X-ray refractive lens at 15 keV



B. Lengeler, M. Richwin, C. Schroer, J. Tümmler,  
RWTH Aachen  
A. Snigirev, I. Snigireva,  
ESRF, Grenoble

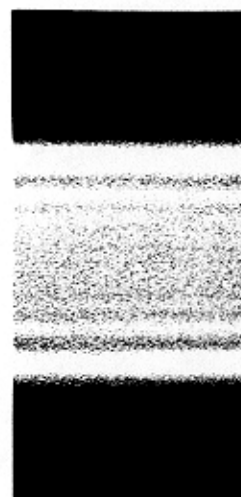
# Fresnel diffraction on the slits / ID22

A. Snigirev, I. Snigireva, V. Kohn, C. Raven (ESRF)

full beam (1 mm)



primary slits (14 m)



200  $\mu\text{m}$



150/100  $\mu\text{m}$

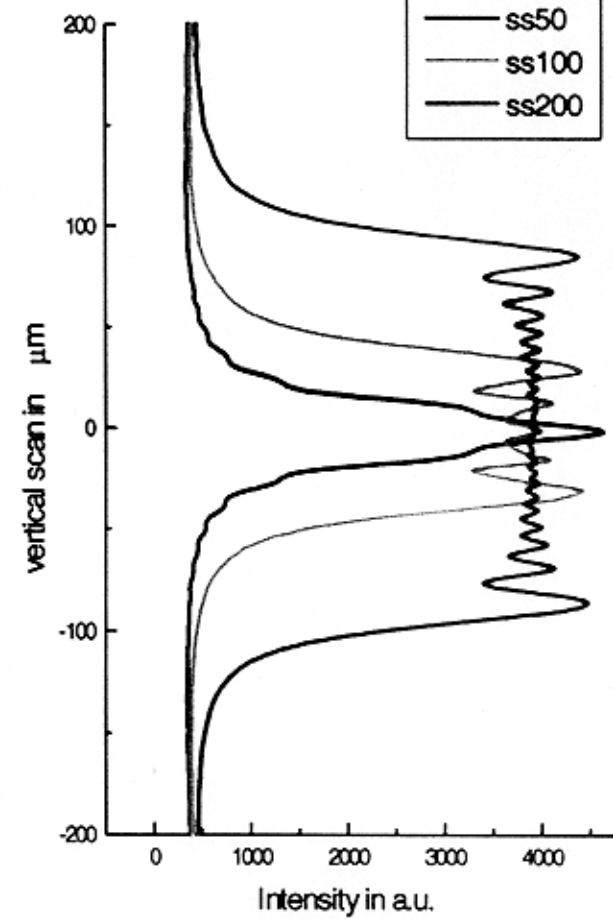


50  $\mu\text{m}$

secondary slits (4.5 m)



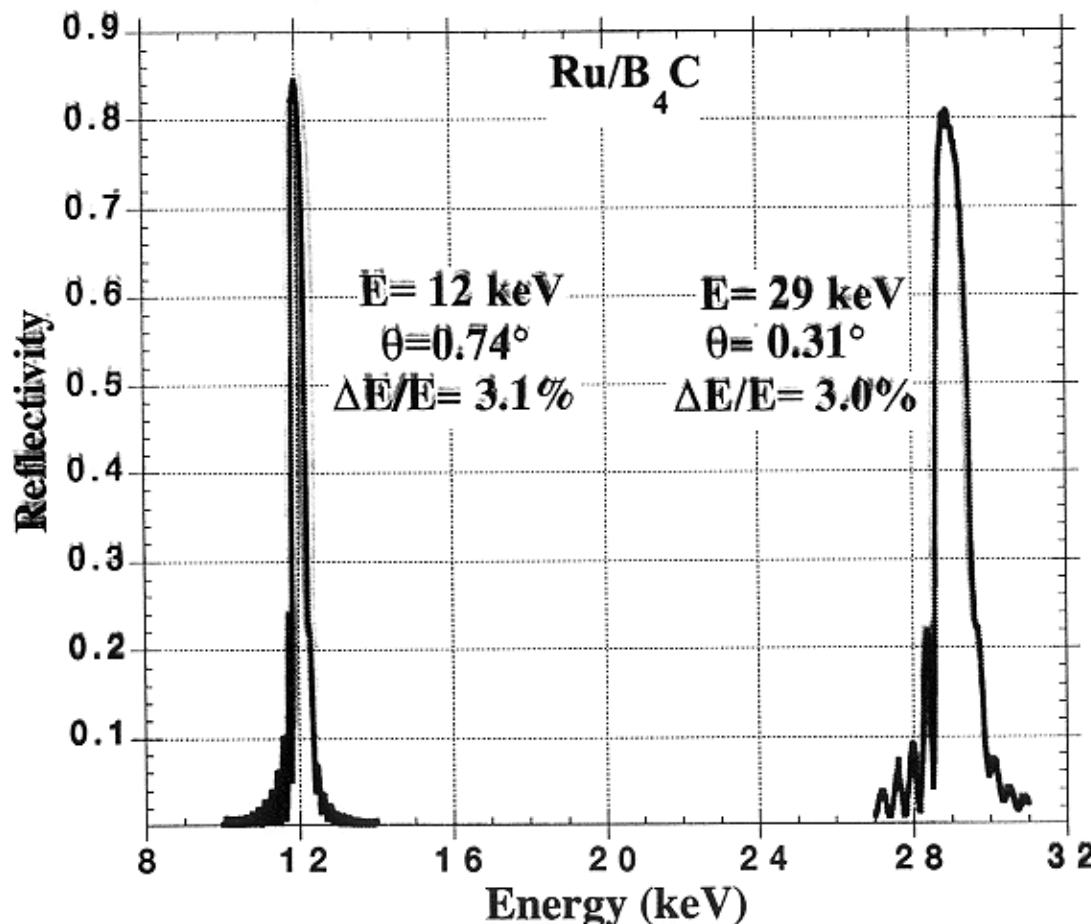
vertical beam intensity  
with secondary slits closed to



# MULTILAYER CHARACTERISTICS

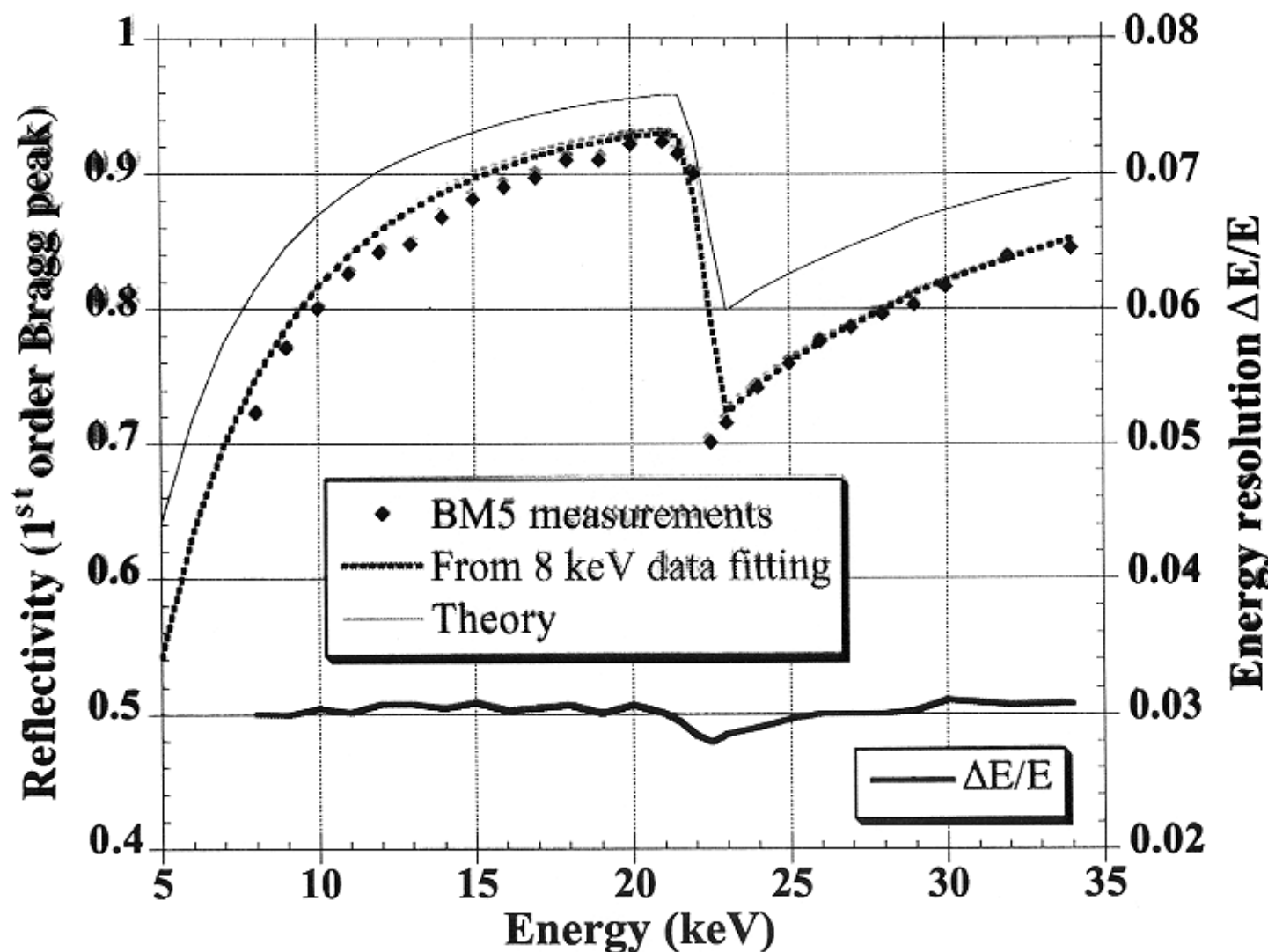
Courtesy: E. HIEGLER, Ch. MOREAU (ESRF)

[Ru/B<sub>4</sub>C]65   d-spacing: 4.19 nm   manufactured at ESRF02  
interface roughness:  $\sigma_{\text{rms}} = 0.25 \text{ nm}$

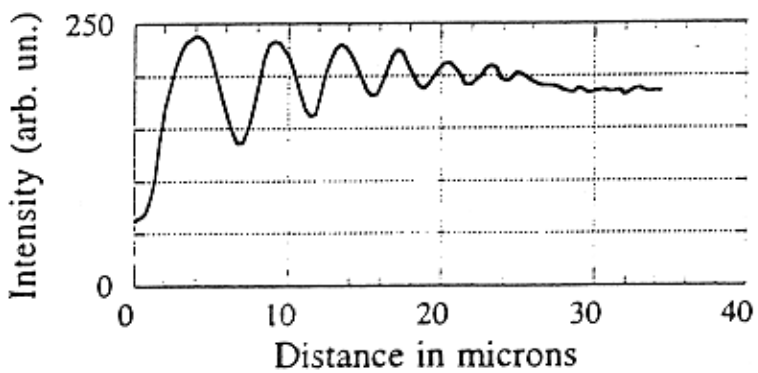
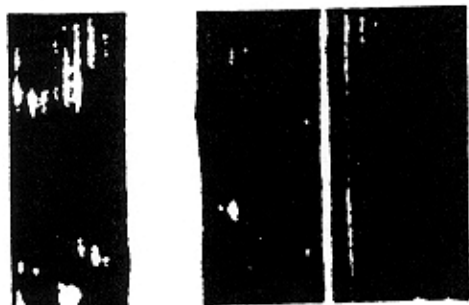
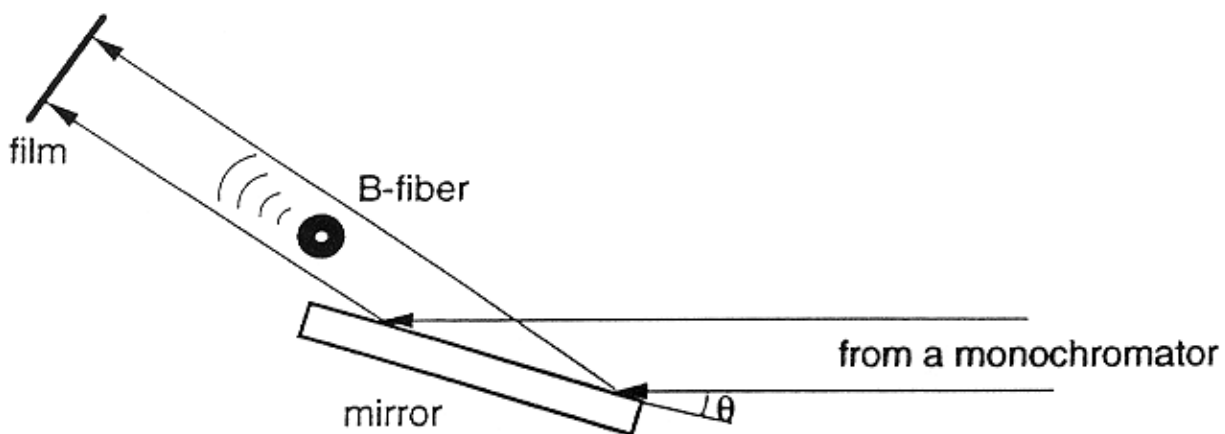
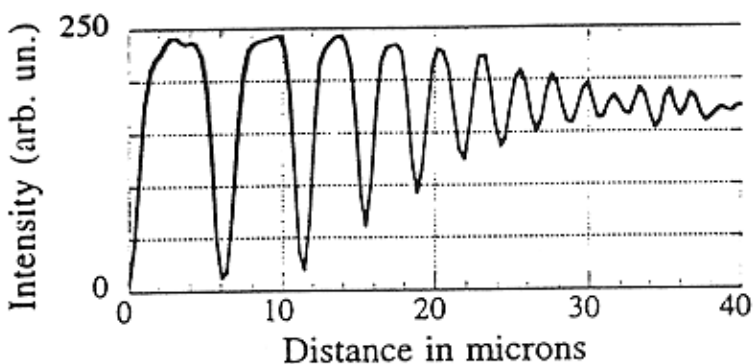
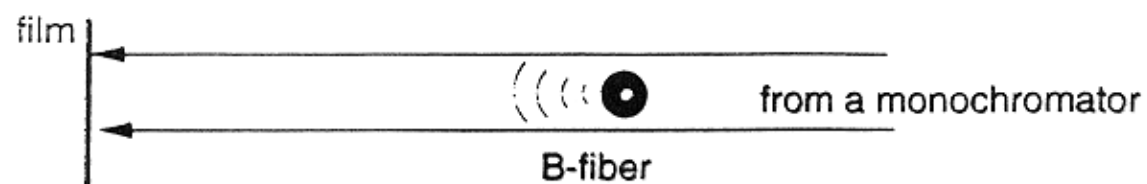


# MULTILAYER PERFORMANCE vs ENERGY

Courtesy: E. ZIEGLER, Ch. MORAWS (ESRF)



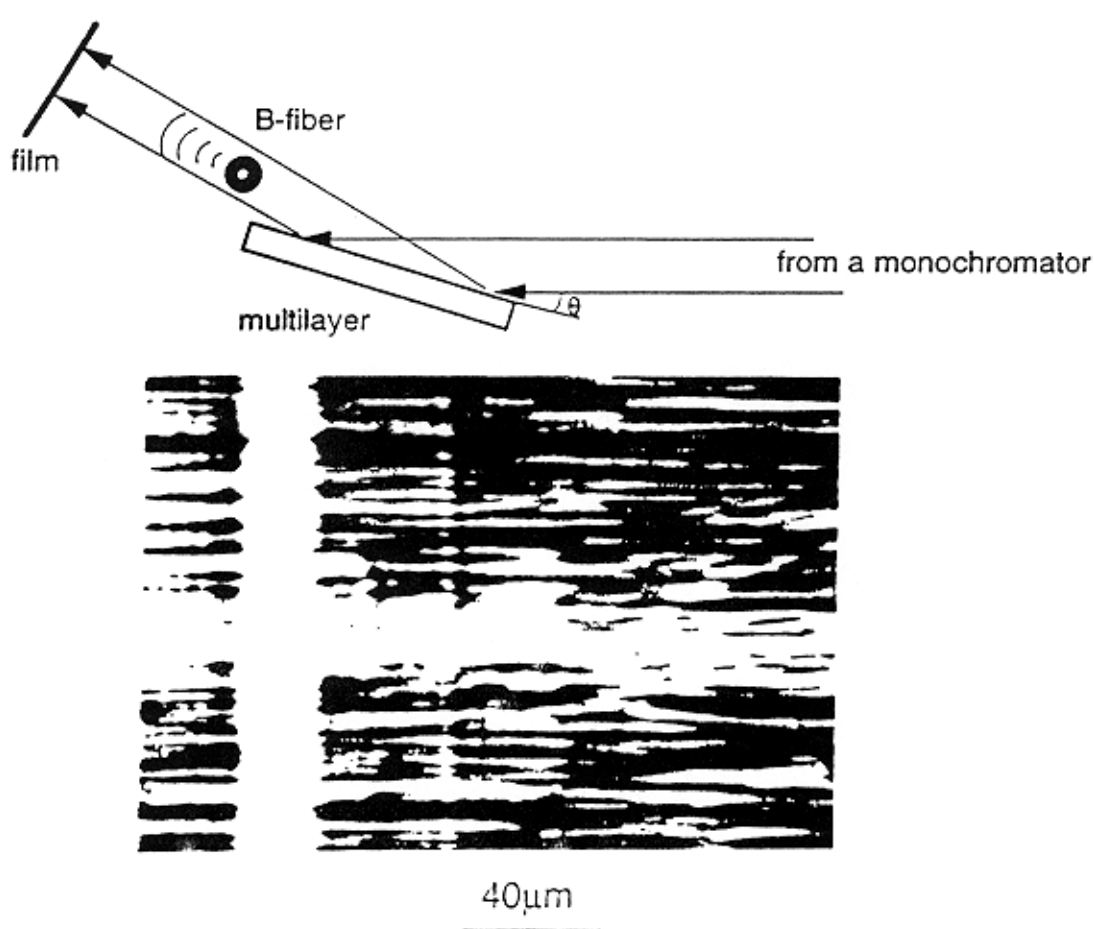
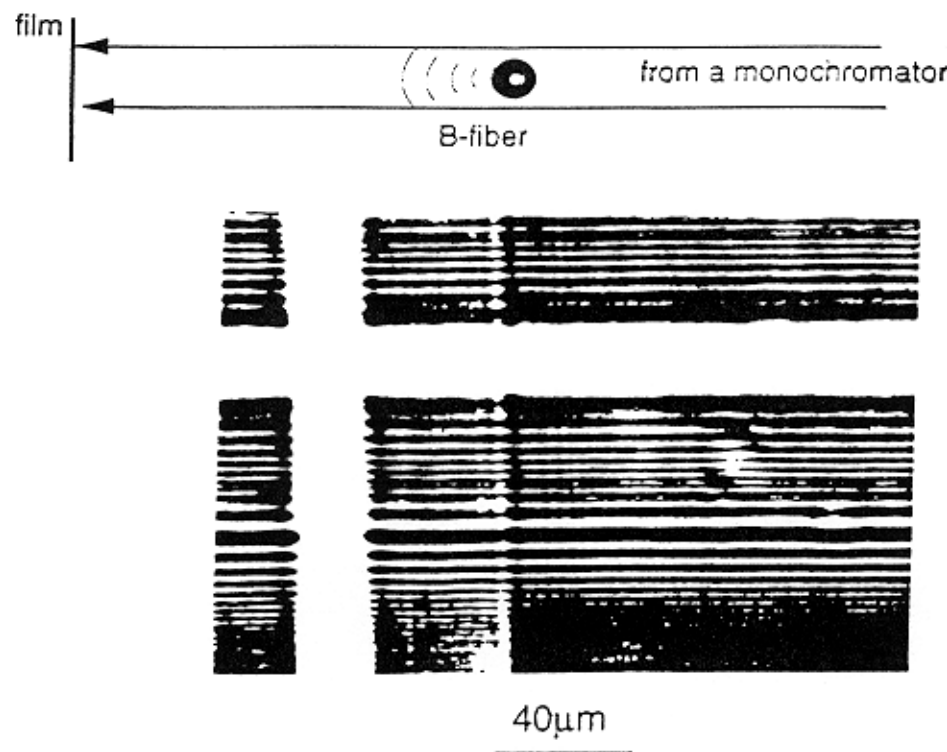
$E=10\text{keV}$   
B-fiber  $\varnothing 100\mu\text{m}$  (W-core  $\varnothing 15\mu\text{m}$ )  
fiber-to-film distance 50cm



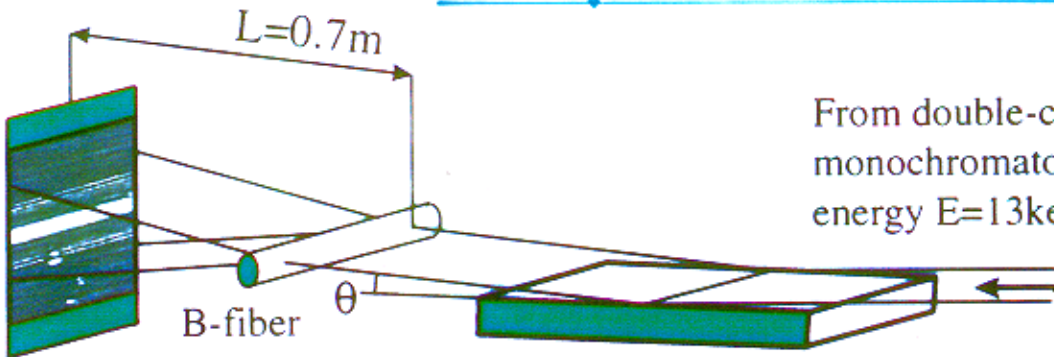
$40\mu\text{m}$

Snigirev et al., 1995.

B-fiber  $\varnothing 100\mu\text{m}$  (W-core  $\varnothing 15\mu\text{m}$ )  
fiber-to-film distance 50cm  
W-Si multilayer  $d=35\text{\AA}$



Courtesy: A. SOUVOROV (ESRF)

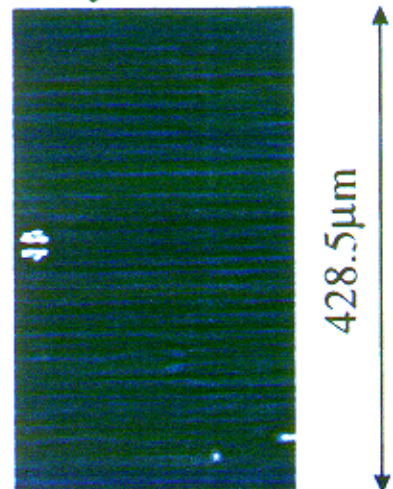


High resolution  
photo film or  
CCD camera

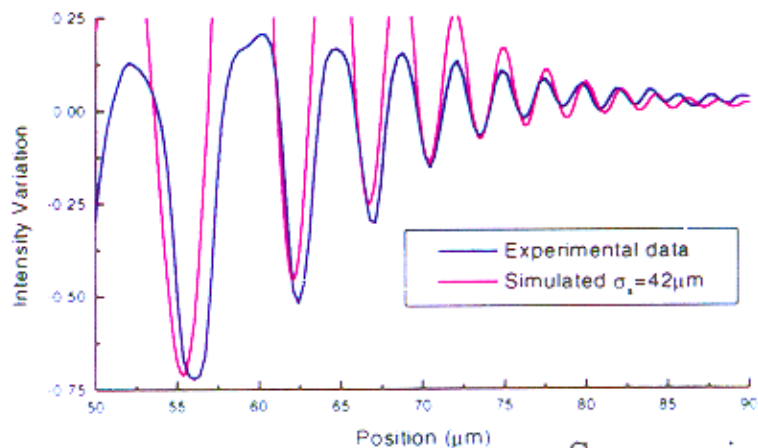
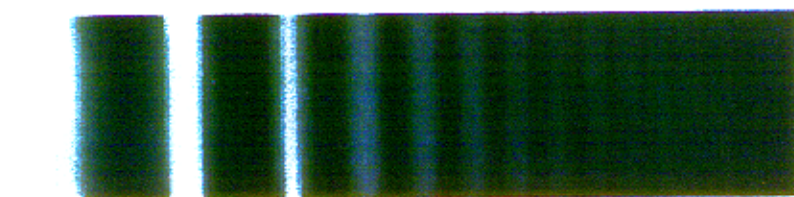
From double-crystal  
monochromator  
energy  $E = 13\text{keV}$

Ru/B<sub>4</sub>C multilayer  
period  $D = 4\text{nm}$ , angle  $\theta = 0.69^\circ$   
number of layers  $N = 60$   
Length/Width  $100 \times 25\text{mm}$

Intensity RMS~10.4%

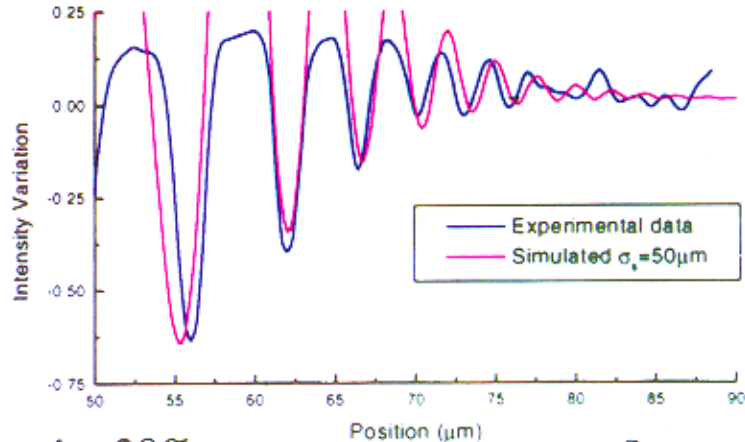
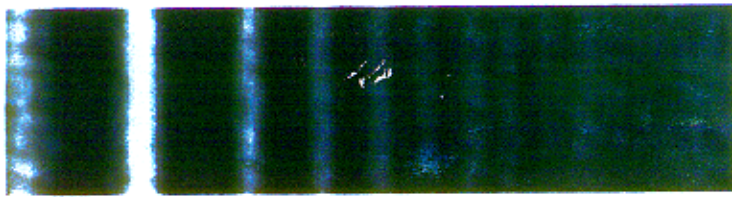


Incident beam

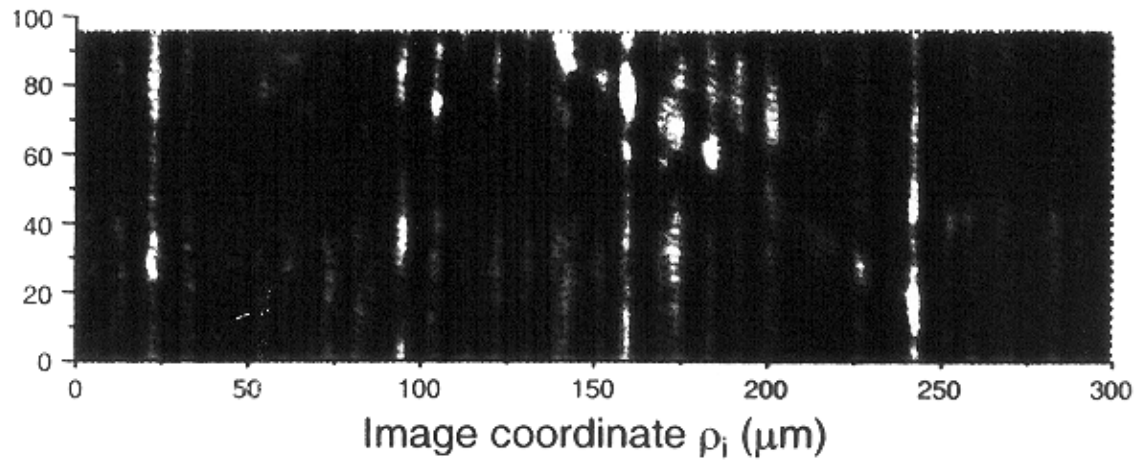


Source size increment by 20%

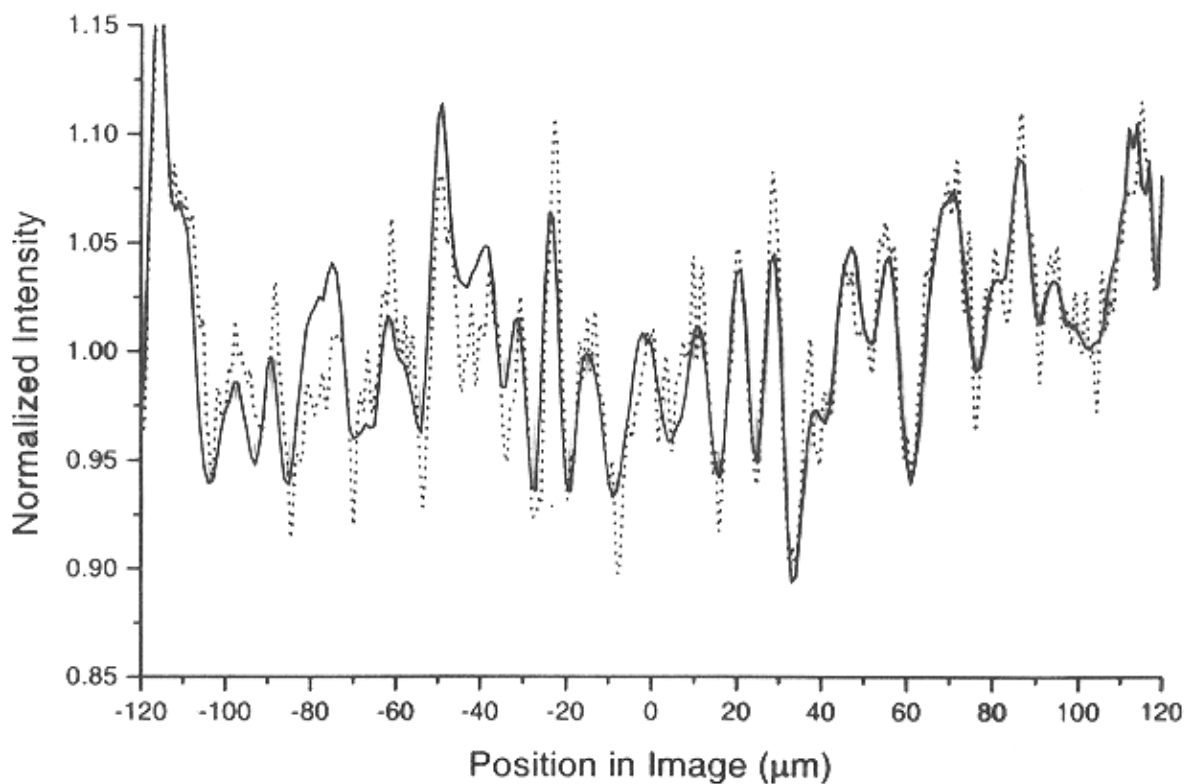
Reflected beam



Souvorov A.



a)



b)

Figure 3